2019

Genetic influence on scar height and pliability after burn injury in individuals of European ancestry: A prospective cohort study

Hilary J. Wallace
The University of Notre Dame Australia, hilary.wallace@nd.edu.au

Gemma Cadby

Phillip E. Melton

Fiona M. Wood

Sian Falder

See next page for additional authors

This article was originally published as:
Wallace, H. J., Cadby, G., Melton, P. E., Wood, F. M., Falder, S., Crowe, M. M., Martin, L. J., Marlow, K., Ward, S. V., & Fear, M. W. (2019). Genetic influence on scar height and pliability after burn injury in individuals of European ancestry: A prospective cohort study. *Burns, 45* (3), 567-578.

Original article available here:
https://doi.org/10.1016/j.burns.2018.10.027

This is the accepted manuscript version of an article published as:

Wallace, H.J., Cadby, G., Melton, P.E., Wood, F.M., Falder, S., Crowe, M.M., Martin, L.J., Marlow, K., Ward, S.V., and Fear, M.W. (2019). Genetic influence on scar height and pliability after burn injury in individuals of European ancestry: A prospective cohort study. *Burns, 45*(3), 567-578. doi: 10.1016/j.burns.2018.10.027

This article has been published in final form at https://doi.org/10.1016/j.burns.2018.10.027

HIGHLIGHTS

- Largest study to date on genetic variants associated with hypertrophic scarring
- No individual gene variants achieved the cut-off threshold of significance
- Nervous system and cell adhesion gene pathways were associated with poor scar outcome

Title: Genetic influence on scar height and pliability after burn injury in individuals of European ancestry: a prospective cohort study

Authors:

*Hilary J Wallace[a,b] (ORCID iD 0000-0002-8370-7647)

Gemma Cadby[c] (ORCID iD 0000-0001-7317-6531)

Phillip E Melton[c,d] (ORCID iD 0000-0003-4026-2964)

Fiona M Wood[a, e] (ORCID iD 0000-0002-3284-6540)

Sian Falder[f]

Margaret M Crowe[e]

Lisa J Martin[e] (ORCID iD 0000-0001-8947-834X)

Karen Marlow[f]

Sarah V Ward[c]

Mark W Fear[a] (ORCID iD 0000-0003-3163-4666)

Affiliations:

[a]Burn Injury Research Unit, School of Biomedical Sciences, Faculty of Health and Medical Sciences, The University of Western Australia, Perth, Australia

[b]School of Medicine, The University of Notre Dame Australia, Fremantle, Australia

[c]Centre for Genetic Origins of Health and Disease, Faculty of Health and Medical Sciences, The University of Western Australia and Faculty of Health Science, Curtin University, Perth, Australia

[d]School of Pharmacy and Biomedical Sciences, Faculty of Health Science, Curtin University, Perth, Australia

[e]Burns Service of Western Australia, Princess Margaret Hospital for Children and Fiona Stanley Hospital, Perth, Australia

[f]Alder Hey Children's NHS Foundation Trust, Liverpool, UK

***Corresponding author:**
Hilary J. Wallace, PhD
School of Medicine

ND18/102

The University of Notre Dame Australia

19 Mouat St (PO Box 1225) Fremantle

Western Australia W 6959

Australia

E-mail address: hilary.wallace@nd.edu.au

ABSTRACT

After similar extent of injury there is considerable variability in scarring between individuals, in part due to genetic factors. This study aimed to identify genetic variants associated with scar height and pliability after burn injury. An exome-wide array association study and gene pathway analysis were performed on a prospective cohort of 665 patients treated for burn injury. Outcomes were scar height (SH) and scar pliability (SP) sub-scores of the modified Vancouver Scar Scale (mVSS). DNA was genotyped using the Infinium® HumanCoreExome-24 BeadChip. Associations between genetic variants (single nucleotide polymorphisms) and SH and SP were estimated using an additive genetic model adjusting for age, sex, number of surgical procedures and % total body surface area of burn in subjects of European ancestry. No individual genetic variants achieved the cut-off threshold of significance. Gene regions were analysed for spatially correlated single nucleotide polymorphisms and significant regions identified using *comb-p* software. This gene list was subject to gene pathway analysis to find which biological process terms were over-represented. Using this approach biological processes related to the nervous system and cell adhesion were the predominant gene pathways associated with both SH and SP. This study suggests genes associated with innervation may be important in scar fibrosis. Further studies using similar and larger datasets will be essential to validate these findings.

KEY WORDS: scars, fibrosis, burn injury, genetic, exome.

ABBREVIATIONS: GO, gene ontology; GWAS, genome-wide association study; HTS, hypertrophic scarring; mVSS, modified Vancouver Scar Scale; PCA, principal component analysis; SH, scar height; SSG, split-thickness skin graft; SNP, single nucleotide polymorphism; SP, scar pliability; %TBSA, % total body surface area of burn

INTRODUCTION

Hypertrophic scarring (HTS) is considered the key unmet challenge after burn injury [1]. Defined as raised scarring that remains within the wound boundary, HTS is the most common complication of burn injury and reported rates vary between 32 and 72% [2]. There is considerable variation in scarring potential between individuals [3], and several lines of evidence support a genetic component to raised skin scars [4]. Identification of genes associated with the increased scar height and reduced pliability may provide insights into the aetiology of excessive dermal fibrosis, which remains poorly understood [5].

Genetic susceptibility to keloid disease (KD), a severe scarring disorder characterized by benign fibroproliferative lesions growing beyond the wound edge, is well-recognized and likely to involve more than one gene [6]. In KD the genetic contribution is indicated by familial aggregation, higher prevalence in certain ethnicities, common occurrence in twins, and alterations in gene expression [7]. Evidence is also emerging of a genetic influence on HTS, with a higher prevalence of hypertrophic surgical scars [8,9] and post-burn scars [10-13] in individuals or ethnic groups with darker skin pigmentation.

A small number of candidate gene studies have examined whether specific single nucleotide polymorphisms (genetic variants) are associated with HTS or poor scar outcome [11,12,14,15]. These have generated limited evidence due to their small size and lack of replication. The low cost of high resolution single nucleotide polymorphism (SNP) arrays means it is now feasible to conduct exome- and genome-wide association studies (GWAS) unconstrained by prior hypotheses [16]; to date one exome-wide association study of post-burn scar outcome has been performed [17]. This study identified one genetic variant (SNP in the *CSMD1* gene (rs11136645) associated with increased scar height in a sample of mixed ancestry [17].

To avoid false positive results in testing hundreds of thousands of SNPs a stringent threshold for significance must be used [18], resulting in sufficient statistical power to identify genetic variants with low to modest effect sizes unless extremely large sample sizes are used [19]. To overcome this issue of multiple-testing, new methods have been recently developed that test for association at a biological (gene) pathway level rather than at the individual SNP level [20], increasing statistical power by reducing the number of tests performed and allowing a functional interpretation of the results [21].

To test the hypothesis that there is a genetic influence on burn scar fibrosis we conducted an exome-wide SNP array association study and gene-based pathway analysis in adults and children who sustained burn injury and were treated at hospital in Western Australia or in Liverpool, United Kingdom. Scar fibrosis is characterised by increased volume and stiffness of collagen within the scar, therefore the two outcome measures for the study were scar height (SH) and scar pliability (SP) sub-scores of the modified Vancouver Scar Scale (mVSS) [22].

MATERIALS AND METHODS

Ethics statements

All adult subjects gave written informed consent and for children under 18 years parents provided written consent (or where applicable the guardian or other primary care giver). Children aged 7 years and above also provided written informed assent. The study was performed according to the Declaration of Helsinki and the National Statement on Ethical Conduct in Human Research 2007 (National Health & Medical Research Council, Australia). Ethical approval was obtained from the Princess Margaret Hospital for Children (Western Australia) Human Research Ethics Committee (Registration Number: 1926/EP), the Research Ethics Committee of the Alder Hey Children's NHS Foundation Trust (Liverpool, United

Kingdom) (REC Reference: 13/NW/0691), Royal Perth Hospital (Western Australia) Human Research Ethics Committee (EC Number: 2009/114) and site authorization from Fiona Stanley Hospital (Western Australia) (Project Number: 2014-105).

Subjects

Adults and children were eligible for recruitment if they sustained an acute burn injury requiring hospital admission, outpatient treatment or HTS treatment in the Burns Service of Western Australia (Royal Perth Hospital, Fiona Stanley Hospital or Princess Margaret Hospital for Children) or at the Alder Hey Children's Hospital (Liverpool, UK). Subjects were recruited in the outpatient clinic or the burns ward. Subjects were excluded if they had a history of more than one hospital admission for acute burn injury, acute burn injury treated outside the Burns Service of Western Australia or Alder Hey Children's Hospital, previous history of keloid scarring, or burn scar diagnosed as a keloid scar. A total of 953 subjects were recruited: 679 adults (Western Australia) and 274 children (Western Australia 244; Liverpool, UK 30).

Patient treatment algorithms

The clinical treatment pathways for patients with burn injury in the care of the Burns Service of Western Australia and Alder Hey Children's Hospital are described in Supplementary Figure S1.

Primary outcome (scar phenotype)

Subjects were followed up for 12 months post-injury with scar assessments conducted according to a modified Vancouver Scar Scale (mVSS) (Figure 1) [22] at 3, 6 and 12 months. The outcome measures were the mVSS scar height (SH: 0 to 4) and scar pliability (SP: 0 to 5) sub-scores of the subject's single 'worst' scar (scar area with the highest total mVSS score) 12 months post-injury. When the 12-month scores were unavailable, the scores closest to 12 months post-injury were used. Scar height (SH) specifically relates to the bulk of the scar above

the level of normal skin and SP is a measure of suppleness. Scar tissue is normally less supple than normal skin because the scar is thicker and has an inferior quality of collagen architecture. Subjects discharged from follow-up prior to 12 months due to 'excellent' scar outcome based on the clinical judgement of a consultant plastic surgeon were assigned SH and SP values of 0. Subjects recruited with prevalent HTS (treated with reconstructive surgery, intra-lesional steroids or laser therapy) were assigned the maximum SH value of 4 and SP value of 5.

Minimum data set

At the time of recruitment data on the following variables was extracted from medical records: age (at time of injury–continuous variable), sex (F; M), external cause of burn injury (scald, contact, flame, sunburn or radiation, chemical, friction, electrical), % total body surface area of burn (%TBSA–continuous variable), length of hospital stay (days), number of surgical procedures (0; 1; more than 1), healed within 14 days (Yes; No).

DNA and genotyping

DNA was collected from subjects using Oragene saliva DNA kits (DNAGenotek, Ottawa, Canada) and extracted and stored in the Western Australian DNA Bank. DNA was genotyped using Infinium® HumanCoreExome-24 v1.1 BeadChip arrays (Illumina Inc., San Diego, CA, USA) at PathWest (Western Australia). This microarray detects both exonic variants (~260,000) and additional intronic and intergenic variants (~240,000 'tag' SNPs).

Statistical analysis

Genotyping and quality control

Of the 953 subjects recruited, 5 did not have DNA collected. DNA from the remaining 948 subjects was genotyped in two batches: Set 1 (n=432); Set 2 (n=516). Batch effects were investigated by performing complete linkage clustering based on pairwise identity by state distance in PLINK, a tool set for whole-genome association and population-based linkage analyses [55]. No batch effects were detected and the two data sets were merged. SNPs were

excluded if they had call rates of less than 95%, minor allele frequencies < 0.1%, or Hardy-Weinberg *P*-values < 1.0×10^{-7}, leaving 298,150 SNPs available for analysis. A total of 283 subjects were removed for the following reasons, leaving 665 subjects for analysis: failed genotyping (no results reported) (n=32); low call rate (<95%) (n=6); sex-ambiguous (n=6); consent incomplete (n=2); keloid scar or history of keloid scar (n=25); missing demographic or clinical information (n=7); missing scar outcome data (n=51); relatedness > 0.125 (n=4); non-CEU (non-European) ancestry (n=150). No individuals had excess SNP heterozygosity.

To account for potential population structure, principal component analysis (PCA) was performed in Eigensoft, software to model ancestry differences [56], using a subset of quality control-filtered SNPs (n = 40,712). The subset of common SNPs (minimum allele frequency [MAF] > 0.1) for PCA was generated using PLINK to compute the genotypic correlation (r^2) between SNP pairs within a 50 SNP window; removing one SNP from a pair of SNPs if r^2> 0.2. Principal component analysis revealed some population structure, and 150 individuals with non-European ancestry were removed; the principal components were retained for use as covariates in subsequent analyses.

Analysis of SNP associations

Associations between each SNP and the two outcomes, SH and SP, were estimated using an additive genetic model. Each outcome was treated as a continuous variable and adjusted by age at time of injury (continuous variable), sex (M; F), number of surgical procedures (0; 1; more than 1), %total body surface area (%TBSA) of the burn and the significant principal components. Model residuals were transformed using the inverse rank Normal transformation and these were used in the genetic analyses. Allelic beta coefficients, 95% confidence intervals (CI) and *P*-values were calculated using multiple linear regression in PLINK. Bonferroni correction for multiple testing was used to account for the number of SNPs tested (298,150),

with *P*-value $<1.7x10^{-7}$ considered statistically significant (critical *P*-value = *a*/n = $0.05/298,150 = <1.7x10^{-7}$).

Statistical power

Supplementary Figure S2 estimates the sample size required to achieve 80% statistical power for differing minor allele frequencies (MAF) and SNP effect sizes. Effect sizes are presented in standard deviation (SD) units. With 665 subjects there is 80% power of detecting a statistically significant association for a SNP with an effect size of ≥ 0.4 and MAF ≥ 0.25. That is, for scar height (SH) and pliability (SP) in this paper, which have standard deviations of ~1.5 (after covariate adjustment), we are powered to detect a SNP (with MAF ≥ 0.25) which resulted in a change of ≥ 0.6 units of SH or SP (1.5 * 0.4). While the effect size per single SNP may differ between ethnicities, the sample size required for each effect size would be consistent across all ethnicities.

Pathway Analysis

To identify genomic regions for pathway analysis, spatially correlated *P*-values were identified using the *comb-p* software package [57]. C*omb-p* identifies genomic regions by 1) calculating the autocorrelation between genetic variants to adjust the resulting *P*-values; 2) running a peak finding algorithm over these adjusted *P*-values to identify enriched regions around a seed signal; and 3) calculating the region *P*-value. A seed signal of *P*-value $<5 \times 10^{-5}$ was used with a distance parameter set to 25 thousand base pairs. Significant gene regions were identified as those with at least two genetic variants sites and *P*-value <0.01. These genomic regions, annotated to the nearest gene, were imported into Pathway Studio® (Elsevier, Netherlands) to identify statistically significant enrichment in genes of known functional groups and curated pathways. Resulting genomic regions were investigated for the Gene Ontology (GO) category, 'biological processes'. Functional pathways were further supported by data extracted from the

literature using MedScan and added in ResNet databases, accessed through the Pathway Studio® interface.

Replication of results from previous studies

Genetic variants reported to have significant association with HTS or raised scar in previous studies were directly compared with this study by 'looking up' the variants in the complete results tables for SH and SP.

RESULTS

Study description and participant characteristics

Exome array SNP genotyping was performed on 948 individuals. Following quality control procedures (including removal of 150 subjects with non-European ancestry), 665 individuals were available for analysis. The median age of the 665 individuals analysed was 27.9 years and 34% of the subjects were female (Table 1). Increased SH and SP were both associated with decreased age, female sex, increased %TBSA and the number of surgeries (all $P<0.01$) (Supplementary Table S1).

Relationship between outcome measures

The outcomes SH, SP and total mVSS score were highly correlated. There were positive linear relationships between SH and SP (Pearson's r=0.905), SH and total mVSS (r=0.91), SP and total mVSS (r=0.91), and [SH+SP] and total mVSS (r=0.94) (Supplementary Figure S3 [a-d]), and also between the model residuals of SH and SP used in the genetic analyses (Supplementary Figure S3 [e]).

Exome-wide association analysis of individual SNPs

The observed distribution of *P*-values for the 298,150 SNPs exhibited minimal deviation from the expected distributions for both outcomes (Supplementary Figure S4). Genomic inflation factors (λ) were calculated by taking the ratio of the median of the observed distribution test

statistics to the expected median. Values greater than 1.10 may indicate evidence of inflation (excess false positives) possibly due to factors such as population stratification (systematic ancestry differences in sub-populations) or cryptic relatedness (kinship in the sample that is not known). No overall inflation of the test statistics for SH or SP were observed, with genomic inflation factors (λ) of 1.00 and 1.01 respectively. The –log10 transformed *P*-values observed across the genome are displayed in Figure 2. No SNPs achieved the Bonferroni-corrected *P*-value threshold of $<1.7 \times 10^{-7}$. The fifty genetic variants with the lowest *P*-values for SH and SP are listed in Table 2 and the complete lists can be viewed in Supplementary Tables S2 (SH) and S3 (SP).

Some variants in Table 2 are associated with genes that could have, or are known to have, a role in skin fibrosis. These include one SNP near activating transcription factor 7 interacting protein 2 (*ATF7IP2*: rs12598337, $P=2.38\times10^{-5}$ [SH]); one SNP near cyclin dependent kinase 8 (*CDK8*: rs1547918, $P=7.60\times10^{-5}$ [SH]); two SNPs in integrin subunit alpha 11 (*ITGA11*: rs898586 [intronic], $P=4.88\times10^{-5}$ [SP]; rs3736493 [synonymous SNP], $P=2.10\times10^{-4}$ [SH]); one SNP near desmoglein 1 (*DSG1*: rs7234316: $P=6.34\times10^{-6}$ [SP]); and one SNP in chemokine (C-C motif) ligand 5 (*CCL5,* also known as *RANTES*: rs1065341 [3' UTR], $P=4.39\times10^{-5}$ [SP]).

Replication of results from previous studies

The *P*-values for genetic variants reported to be associated with HTS or increased scar height in previous studies are reported in Table 3. SNPs in the *CSMD1* (rs11136645) [17] and *PTPN5* (rs56234898) [14] genes were not significantly associated with SH or SP in the present study, nor did they approach the threshold *P*-value. To test the reported association with *HLA-DRB1*16* [23], a tag SNP of this allele was examined (rs6923504), but was not significant. No SNPs in the *TGFB1* gene [15] were significantly associated with SH or SP (all $P>0.01$). Similarly, no SNPs in the melanocortin 1 receptor (*MC1R*) gene [11] were significantly associated with SH or SP (all $P>0.01$).

Gene Pathway Analysis

None of the individual SNPs achieved the threshold *P*-value and pathway analysis was therefore used as this consolidates the effects of multiple variants in genomic regions and increases the power of the study. A total of 45 significant enriched GO 'biological process' pathways were less than the Bonferroni-corrected *P*-value threshold of $P<1.68x10^{-6}$ (29,656 gene ontology (GO) pathways). Significant enriched 'biological process' GO terms for both scar outcomes, SH (n=19 terms) and SP (n=26 terms), are listed in Table 4. The lists of overlapping gene entities in the significant pathways are available in Supplementary Tables S4 (SH) and S5 (SP). The scope of the top ten enriched terms was similar for both outcomes. Three pathways involving the nervous system were present in the top ten of both outcome lists: *nervous system* development (SH $P<3.42x10^{-14}$; SP $P<2.41x10^{-17}$), *axon guidance* (SH $P<2.95x10^{-17}$; SP $P<2.30x10^{-10}$) and *synaptic transmission* (SH $P<5.78x10^{-13}$*;* SP $P<1.34x10^{-11}$*)*. Several other pathways were related to cell to cell communication and cell adhesion. The term, *cell adhesion,* was present in both outcome lists, and *homophilic cell adhesion via plasma membrane adhesion molecules*, *cell-cell junction assembly*, *cell junction assembly* and *single organismal cell-cell adhesion* were present in the SP outcome list. The term, *extracellular matrix organisation,* was present in the SH outcome list.

DISCUSSION

This study has applied association and biological pathway analysis to a human exome array study focussed on identifying variants associated with raised scar after burn injury. Using this approach the predominant biological process pathways associated with SH and SP were those related to the nervous system and to cell adhesion.

No significant associations of individual SNPs reported in previous studies were replicated in this study. These include a SNP in the *CSMD1* gene (rs11136645) reported in a study using the

same exome array and a similar scar outcome measure of scar height [17]. The latter does not include access to the complete results tables or provision for data sharing to enable comparisons to be made with other genetic variants of interest. The failure to replicate results of individual genetic variants in independently conducted studies largely points to the low statistical power of all studies conducted to date. Sample size has ranged from 128 to 538 for candidate SNP studies, and 538 [17] to 665 (present study) for exome-wide studies. Statistical power is influenced by the characteristics of the phenotype and the putative genetic variant [24], with small sample size limiting the power of gene association tests for genes of modest effect size.

In this study no individual SNPs achieved the Bonferroni-corrected *P*-value threshold, due to the relatively small number of samples when investigating a large number of SNPs. While this study did not identify any genome-wide significant variants after multiple correction, a few variants from Table 2 are notable due to their association with genes that have functions that could be connected with fibrosis. *ATF7IP 2* regulates gene transcription and chromatin formation [25,26] and *CDK8* drives a cycle of Smad utilization and disposal that is an integral part of canonical TGF-β signalling pathways [27] which promote fibrosis. *ITGA11* is expressed in dermal fibroblasts [28] where it contributes to collagen type I binding and collagen production [29,30]. A gene closely related to *DSG1*, *DSG2*, is involved in cardiac fibrosis [31] and *CCL5* (RANTES) is a chemokine which appears to mediate important aspects of fibrosis in liver disease [32].

Pathway analysis was conducted to increase the power of the study, by consolidating the effect of sets of individual SNPs located in the same gene region [21]. Grouping sets of individual SNPs may identify pathways that are significantly associated with SH or SP even if individual SNPs are not significantly associated. The finding that three of the top ten enriched GO terms relate to the nervous system is of interest. The term *nervous system development* is a broad

term and includes responses that occur after peripheral nerve injury from burn – for example, nerve fibre regrowth. After burn injury there is an initial loss of nerve fibres in the skin followed by skin reinnervation during wound healing [33]. However in the long-term scar tissue has reduced nerve density compared to uninjured skin [34-36]. The term *axon guidance* refers to the process that guides axon migration to a specific target site in response to attractive and repulsive cues. Axon guidance cues include the Eph receptor family and their ligands, Ephrins, which have been shown to play an important role in cutaneous innervation during development [37,38] and to be regulated by skin wounding [37]. The term *synaptic transmission* relates to the biological process by which a nerve cell communicates with a target cell across a synapse. Peripheral nerve injury in partial and full-thickness burns [39] may lead to neuropathic pain [40], believed to be caused by maladaptive changes at synaptic level (spinal and supra-spinal) [41].

The findings suggest that pathways related to nervous system function may influence the extent of scar fibrosis. It is known that peripheral nerve fibres and central mechanisms are closely linked to inflammatory and immune responses [42-44] and nerves can enhance wound repair [45,46]. Deficiencies in mechanosignalling pathways [47] and hyperreactivity or derangement of the mechanosensitive nociceptors of nerve fibres [48] have been suggested to contribute to HTS formation, which may be mediated by neurogenic inflammation [49]. Reconstitution of lost body parts and tissue remodelling in various animal species is dependent on functional innervation [50]. The axon guidance cues, Eph receptors and Ephrins, have a role in regulating keratinocyte migration, differentiation and proliferation [51] which may influence wound repair. Ephrin signalling may also have a role in the dermis, but presently the information regarding a role for specific Eph/Ephrin molecules in the dermis is more limited [52].

The term *cell adhesion* is the attachment of a cell, either to another cell or to an underlying substrate such as the extracellular matrix (ECM), via cell adhesion molecules. The importance

of cell/ECM interactions in scar outcome is well recognised with ECM glycoproteins, ligands, integrins, and the cytoskeleton forming a finely tuned network [53]. The finding that *cell adhesion* was one of the top pathways for both SH and SP is therefore consistent with the literature and helps to validate the results of the pathway analysis. Similarly, the presence of the term, *extra cellular matrix organisation*, a process key to the height of scars, in the SH outcome list, is an expected result that supports the validity of the study approach.

To our knowledge this represents the largest association study performed to date for burn scar outcome adjusted for known confounders that may be associated with HTS. It used reliable and defined outcome measures that are directly associated with the extent of dermal fibrosis, height (SH) and pliability (SP) of the subject's 'worst' scar [54]. While the study is not adequately powered for analysis at genetic variant level, a biological pathway analysis was also employed.

The key limitation of the study is small sample size, but another relates to incomplete adjustment for non-genetic factors in the analysis. Further limitations include the variable 'surgery number' being collected at subject level rather than scar level, and the 'worst' scar area being identified according to total mVSS score rather than SH or SP. The influence of scar therapies (pressure garments, massage, silicone) was not accounted for in the analysis, and the analysis was restricted to subjects of European ancestry. Further studies using similar and larger datasets will be essential to validate these findings.

The challenges in recruiting sufficient subjects with a history of burn injury from single centres means that multi-centre studies are essential to achieve the sample sizes required for adequately-powered genetic studies focused on wound healing/repair. These studies will require harmonised study methodologies with reliable outcome measurements and data-sharing protocols. The data from this study suggest a novel role of the nervous system in influencing

dermal fibrosis and will make an important contribution to future meta-analyses. Hypotheses related to the role of the nervous system in dermal fibrosis after burn injury can be explored by developing and testing novel mechanisms *in vitro* and *in vivo*.

Data availability

All data generated during this study are included in this published article (and its Supplementary Information files). The individual-level genotype and phenotype data analysed during the current study are available from the corresponding author on reasonable request.

COMPETING INTERESTS

The authors have no competing financial interests to declare.

DISCLOSURE OF FUNDING

This study was supported by a Wound Management Innovation Cooperative Research Centre (Australia) project grant (Project 1-03), the Fiona Wood Foundation and The University of Western Australia. MWF is supported by Chevron Australia and HJW, MMC and LJM by the Fiona Wood Foundation. The authors also acknowledge support from the Royal Perth Hospital Medical Research Foundation. These funding bodies had no role in the design of the study, the collection, analysis, interpretation of data or writing the manuscript.

AUTHOR CONTRIBUTIONS

HJW and MWF made substantial contributions to study conception and design, interpretation of data and drafting the article. GC and PEM made substantial contributions to study conception and design, analysis and interpretation of data and drafting the article. FMW and SF made substantial contributions to the study conception and design and revising the article critically for important intellectual content. LJM, MMC and KM made substantial contributions to the acquisition of data and revising the article critically for important intellectual content. SVW made a substantial contribution to the interpretation of data and revising the article critically for important intellectual content. All authors approved of final version to be published.

ACKNOWLEDGEMENTS

The authors thank Ms Anne Henderson, Ms Helen deJong and Dr Uliya Gankande for performing the scar assessments.

REFERENCES

[1] Finnerty CC, Jeschke MG, Branski LK, Barret JP, Dziewulski P, Herndon DN. Hypertrophic scarring: the greatest unmet challenge after burn injury. Lancet 2016;388(10052):1427-36.

[2] Lawrence JW, Mason ST, Schomer K, Klein MB. Epidemiology and impact of scarring after burn injury: a systematic review of the literature. J Burn Care Res 2012;33(1):136-46.

[3] Bayat A, McGrouther DA, Ferguson MW. Skin scarring. BMJ 2003;326(7380):88-92.

[4] Brown JJ, Bayat A. Genetic susceptibility to raised dermal scarring. Br J Dermatol 2009;161(1):8-18.

[5] Gardet A, Zheng TS, Viney JL. Genetic architecture of human fibrotic diseases: disease risk and disease progression. Front Pharmacol 2013;4:159.

[6] Shih B, Bayat A. Genetics of keloid scarring. Arch Dermatol Res 2010;302(5):319-39.

[7] Halim AS, Emami A, Salahshourifar I, Kannan TP. Keloid scarring: understanding the genetic basis, advances, and prospects. Arch Plast Surg 2012;39(3):184-9.

[8] Li-Tsang CW, Lau JC, Chan CC. Prevalence of hypertrophic scar formation and its characteristics among the Chinese population. Burns 2005;31(5):610-6.

[9] Soltani AM, Francis CS, Motamed A, Karatsonyi AL, Hammoudeh JA, Sanchez-Lara PA, et al. Hypertrophic scarring in cleft lip repair: a comparison of incidence among ethnic groups. Clin Epidemiol 2012;4:187-91.

[10] Goei H, van der Vlies CH, Hop MJ, Tuinebreijer WE, Nieuwenhuis MK, Middelkoop E, et al. Long-term scar quality in burns with three distinct healing potentials: A multicenter prospective cohort study. Wound Repair Regen 2016;24(4):721-30.

[11] Sood RF, Hocking AM, Muffley LA, Ga M, Honari S, Reiner AP, et al. Race and melanocortin 1 receptor polymorphism R163Q are associated with post-burn hypertrophic scarring: A prospective cohort study. J Invest Dermatol 2015;135(10):2394-401.

[12] Thompson CM, Hocking AM, Honari S, Muffley LA, Ga M, Gibran NS. Genetic risk factors for hypertrophic scar development. J Burn Care Res 2013;34(5):477-82.

[13] Wallace HJ, Fear MW, Crowe M, Martin L, Wood FM. Identification of factors predicting scar outcome after burn injury in adults: a prospective case-control study. Burns 2017;43**:**1271-83.

[14] Sood RF, Arbabi S, Honari S, Gibran NS. Missense variant in MAPK inactivator PTPN5 is associated with decreased severity of post-burn hypertrophic scarring. PloS One 2016;11(2):e0149206.

[15] Ward SV, Cadby G, Heyworth JS, Fear MW, Wallace HJ, Cole JM, et al. Association of TGFbeta1 and clinical factors with scar outcome following melanoma excision. Arch Dermatol Res 2012;304(5):343-51.

[16] Hirschhorn JN, Daly MJ. Genome-wide association studies for common diseases and complex traits. Nat Rev Genet 2005;6(2):95-108.

[17] Sood RF, Hocking AM, Muffley LA, Ga M, Honari S, Reiner AP, et al. Genome-wide association study of postburn scarring identifies a novel protective variant. Ann Surg 2015;262(4):563-9.

[18] Johnson RC, Nelson GW, Troyer JL, Lautenberger JA, Kessing BD, Winkler CA, et al. Accounting for multiple comparisons in a genome-wide association study (GWAS). BMC Genomics 2010;11:724.

[19] Wang K, Li M, Hakonarson H. Analysing biological pathways in genome-wide association studies. Nature Rev Genet 2010;11(12):843-54.

[20] Gui H, Li M, Sham PC, Cherny SS. Comparisons of seven algorithms for pathway analysis using the WTCCC Crohn's Disease dataset. BMC Res Notes 2011;4:386.

[21] Wu MC, Kraft P, Epstein MP, Taylor DM, Chanock SJ, Hunter DJ, et al. Powerful SNP-set analysis for case-control genome-wide association studies. Am J Hum Genet 2010;86(6):929-42.

[22] Baryza MJ, Baryza GA. The Vancouver Scar Scale: an administration tool and its interrater reliability. J Burn Care Rehabil 1995;16(5):535-8.

[23] Castagnoli C, Peruccio D, Stella M, Magliacani G, Mazzola G, Amoroso A, et al. The HLA-DR beta 16 allogenotype constitutes a risk factor for hypertrophic scarring. Hum Immunol 1990;29(3):229-32.

[24] Sham PC, Purcell SM. Statistical power and significance testing in large-scale genetic studies. Nature Rev Genet 2014;15(5):335-46.

[25] Fujita N, Watanabe S, Ichimura T, Ohkuma Y, Chiba T, Saya H, et al. MCAF mediates MBD1-dependent transcriptional repression. Mol Cell Biol 2003;23(8):2834-43.

[26] Wang H, An W, Cao R, Xia L, Erdjument-Bromage H, Chatton B, et al. mAM facilitates conversion by ESET of dimethyl to trimethyl lysine 9 of histone H3 to cause transcriptional repression. Mol Cell 2003;12(2):475-87.

[27] Alarcon C, Zaromytidou AI, Xi Q, Gao S, Yu J, Fujisawa S, et al. Nuclear CDKs drive Smad transcriptional activation and turnover in BMP and TGF-beta pathways. Cell 2009;139(4):757-69.

[28] Barczyk MM, Olsen LH, da Franca P, Loos BG, Mustafa K, Gullberg D, et al. A role for alpha11beta1 integrin in the human periodontal ligament. J Dent Res 2009;88(7):621-6.

[29] Gardner H, Kreidberg J, Koteliansky V, Jaenisch R. Deletion of integrin alpha 1 by homologous recombination permits normal murine development but gives rise to a specific deficit in cell adhesion. Dev Biol 1996;175(2):301-13.

[30] Gardner HA. Integrin signaling in fibrosis and scleroderma. Curr Rheumatol Rep 1999;1(1):28-33.

[31] Pilichou K, Nava A, Basso C, Beffagna G, Bauce B, Lorenzon A, et al. Mutations in desmoglein-2 gene are associated with arrhythmogenic right ventricular cardiomyopathy. Circulation 2006;113(9):1171-9.

[32] Sahin H, Wasmuth HE. Chemokines in tissue fibrosis. Biochim Biophys Acta 2013;1832(7):1041-8.

[33] Kishimoto, S. The regeneration of substance P-containing nerve fibers in the process of burn wound healing in the guinea pig skin. J Invest Dermatol 1984;83:219-23.

[34] Altun V, Hakvoort TE, van Zuijlen PP, van der Kwast TH, Prens EP. Nerve outgrowth and neuropeptide expression during the remodeling of human burn wound scars. A 7-month follow-up study of 22 patients. Burns 2001;27(7):717-22.

[35] Anderson JR, Zorbas JS, Phillips JK, Harrison JL, Dawson LF, Bolt SE, et al. Systemic decreases in cutaneous innervation after burn injury. J Invest Dermatol 2010;130(7):1948-51.

[36] Nedelec B, Hou Q, Sohbi I, Choiniere M, Beauregard G, Dykes RW. Sensory perception and neuroanatomical structures in normal and grafted skin of burn survivors. Burns 2005;31(7):817-30.

[37] Moss A, Alvares D, Meredith-Middleton J, Robinson M, Slater R, Hunt SP, et al. Ephrin-A4 inhibits sensory neurite outgrowth and is regulated by neonatal skin wounding. Eur J Neurosci 2005;22(10):2413-21.

[38] Wijeratne DT, Rodger J, Wallace HJ, Maghami S, Sykes M, Wood FM, et al. Ephrin-A2 and Ephrin-A5 are important for the functional development of cutaneous innervation in a mouse model. J Invest Dermatol 2015;135(2):632-5.

[39] Coert JH. Pathophysiology of nerve regeneration and nerve reconstruction in burned patients. Burns 2010;36(5):593-8.

[40] Schneider JC, Harris NL, El Shami A, Sheridan RL, Schulz JT, 3rd, Bilodeau ML, et al. A descriptive review of neuropathic-like pain after burn injury. J Burn Care Res 2006;27(4):524-8.

[41] Rohampour K, Azizi H, Fathollahi Y, Semnanian S. Peripheral nerve injury potentiates excitatory synaptic transmission in locus coeruleus neurons. Brain Res Bull 2017;130:112-7.

[42] Scott JR, Muangman P, Gibran NS. Making sense of hypertrophic scar: a role for nerves. Wound Repair Regen 2007;15 Suppl 1:S27-31.

[43] Shepherd AJ, Downing JE, Miyan JA. Without nerves, immunology remains incomplete -in vivo veritas. Immunology 2005;116(2):145-63.

[44] Torii H, Tamaki K, Granstein RD. The effect of neuropeptides/hormones on Langerhans cells. J Dermatol Sci 1998;20(1):21-8.

[45] Ashrafi M, Baguneid M, Bayat A. The role of neuromediators and innervation in cutaneous wound healing. Acta Derm Venereol 2016;96(5):587-94.

[46] Harsum S, Clarke JD, Martin P. A reciprocal relationship between cutaneous nerves and repairing skin wounds in the developing chick embryo. Dev Biol 2001;238(1):27-39.

[47] Huang C, Akaishi S, Ogawa R. Mechanosignaling pathways in cutaneous scarring. Arch Dermatol Res 2012;304(8):589–97.

[48] Akaishi S, Ogawa R, Hyakusoku H. Keloid and hypertrophic scar: neurogenic inflammation hypotheses. Med Hypotheses 2008;71(1):32–8.

[49] Ogawa R, Hsu CK. Mechanobiological dysregulation of the epidermis and dermis in skin disorders and in degeneration. J Cell Mol Med 2013;17(7):817-22.

[50] Boilly B, Faulkner S, Jobling P, Hondermarck H. Nerve dependence: from regeneration to cancer. Cancer Cell 2017;31(3):342-54.

[51] Wijeratne DT, Rodger J, Wood FM, Fear MW. The role of Eph receptors and Ephrins in the skin. Int J Dermatol 2016;55(1):3-10.

[52] Avouac J, Clemessy M, Distler JH, Gasc JM, Ruiz B, Vacher-Lavenu MC, et al. Enhanced expression of ephrins and thrombospondins in the dermis of patients with early diffuse systemic sclerosis: potential contribution to perturbed angiogenesis and fibrosis. Rheumatology 2011;50(8):1494-504.

[53] Widgerow AD. Cellular/extracellular matrix cross-talk in scar evolution and control. Wound Repair Regen 2011;19(2):117-33.

[54] Gankande TU, Wood FM, Edgar DW, Duke JM, DeJong HM, Henderson AE, et al. A modified Vancouver Scar Scale linked with TBSA (mVSS-TBSA): Inter-rater reliability of an innovative burn scar assessment method. Burns 2013;39(6):1142-9.

[55] Purcell S, Neale B, Todd-Brown K, Thomas L, Ferreira MA, Bender D, et al. PLINK: a tool set for whole-genome association and population-based linkage analyses. Am J Hum Genet 2007;81(3):559-75.

[56] Price AL, Patterson NJ, Plenge RM, Weinblatt ME, Shadick NA, Reich D. Principal components analysis corrects for stratification in genome-wide association studies. Nat Genet 2006;38(8):904-9.

[57] Pedersen BS, Schwartz DA, Yang IV, Kechris KJ. Comb-p: software for combining, analyzing, grouping and correcting spatially correlated P-values. Bioinformatics 2012;28(22):2986-8.

[58] de Bakker PI, McVean G, Sabeti PC, Miretti MM, Green T, Marchini J, et al. A high-resolution HLA and SNP haplotype map for disease association studies in the extended human MHC. Nat Genet 2006;38(10):1166-72.

FIGURE LEGENDS

Figure 1. Modified Vancouver Scar Scale [22].

Figure 2. Manhattan plots of genotyped SNPs from additive genetic model: (a) scar height (SH); (b) scar pliability (SP). The –log10 transformed *P*-values observed across the genome are displayed. No SNPs achieved the threshold *P*-value of $<1.7 \times 10^{-7}$.

Pigmentation
0 = normal 1 = hypopigmentation 2 = mixed pigmentation 3 = hyperpigmentation
Vascularity
0 = normal 1 = pink 2 = red 3 = purple
Pliability
0 = normal 1 = supple – flexible with minimal resistance 2 = yielding – giving way to pressure 3 = firm – inflexible, not easily moved, resistant to manual pressure 4 = banding –rope-like tissue that blanches with extension of scar 5 = contracture – permanent shortening of scar producing deformity or distortion
Height
0 = normal – flat 1 = 0 to 1 mm 2 = 1 to 2 mm 3 = 2 to 4 mm 4 = > 4 mm

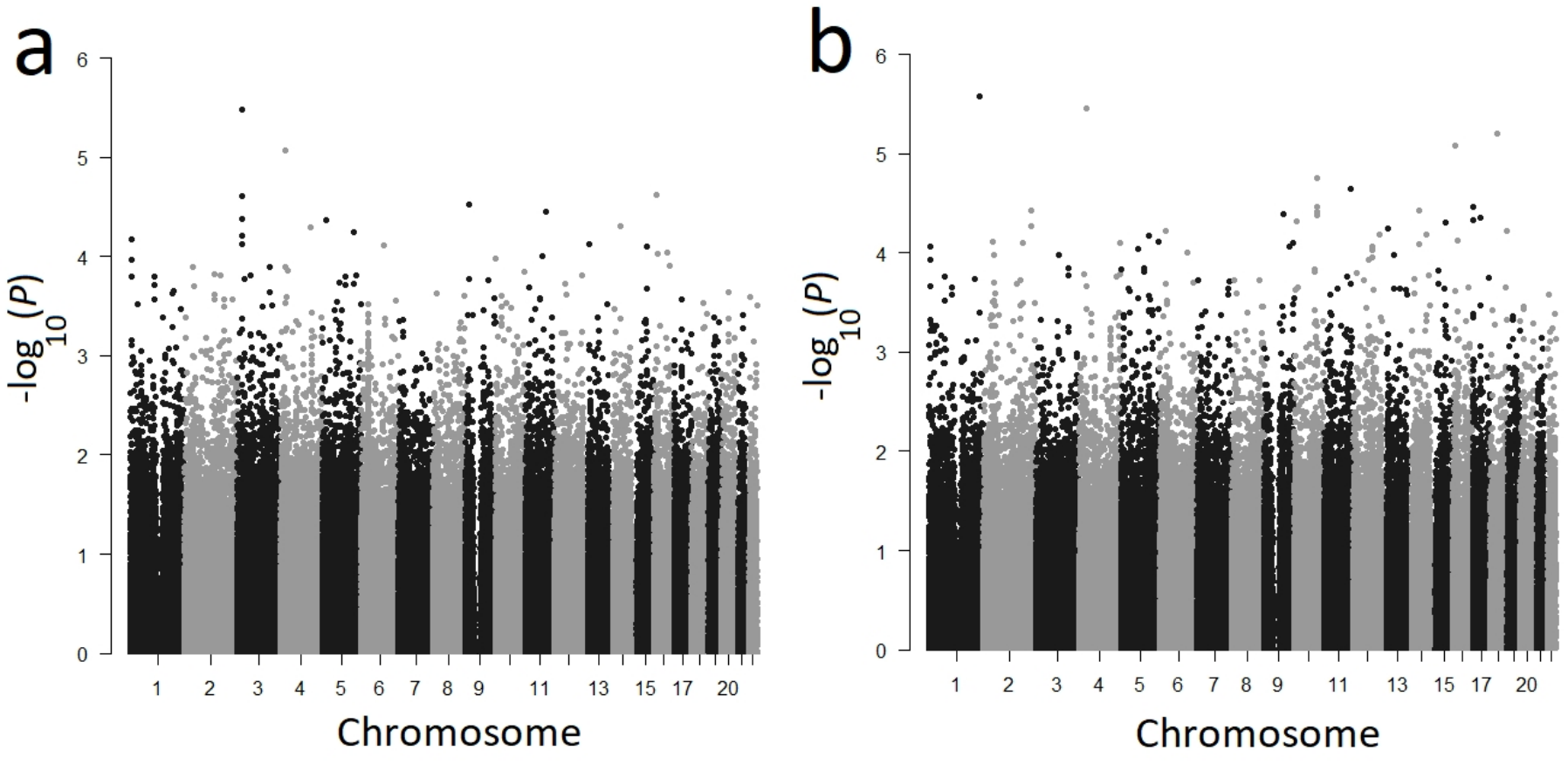
a
b
-log10 (P)
0
1
2
3
4
5
6
1
2
3
4
5
6
7
8
9
11
13
15
17
20
Chromosome

Table 1. The characteristics of subjects included in the analysis (n=665).

Categorical variables		**% (n)**
Male sex		66.2 (440)
Wound Complications (yes)		27.7 (180)
Reconstructive surgery (yes)		16.3 (107)
Multiple surgical procedures (>1)		16.2 (108)
Healed in 14 days (yes)		30.1 (179)
Asthma (yes)		13.7 (91)
Eczema (yes)		6.6 (44)
Diabetes (Type I or II) (yes)		5.3 (35)
Fitzpatrick skin type	1	2.3 (15)
	2	33.4 (219)
	3	53.3 (349)
	4	9.9 (65)
	5	0.9 (6)
	6	0.2 (1)
External cause of burn	Flame	42.1 (280)
	Contact	21.1 (140)
	Scald	29.5 (196)
	Sunburn or radiation	0.6 (4)
	Chemical	4.4 (29)
	Friction	1.9 (13)
	Electrical	0.4 (3)
Burn location	Face/head/neck	3.3 (22)
	Chest/ abdomen/groin	11.2 (74)
	Back/buttocks	4.7 (31)
	Arm	27.9 (185)
	Hand	9.2 (61)
	Leg	35.6 (236)
	Foot	7.9 (52)
	Genitalia	0.2 (1)
Surgery Level	Conservative	18.8 (124)
	ReCell only	17.8 (118)
	SSG ± ReCell	61.9 (409)
	Integra (+SSG+ReCell)	1.5 (10)
Continuous variables		**Median (IQR)**
Age (years)		27.9 (15.6 – 46.7)
TBSA (%)		3 (1-7)
Length of hospital stay (days)		5 (1-12)
Time from burn to scar exam (months)		10.40 (5.80 – 13.95)
Scar height (mVSS score)		1 (0-1)
Scar pliability (mVSS score)		0 (0-2)
Total mVSS score		4 (3-8)

Table 2. The top fifty genetic variants associated with scar height and pliability (smallest *P*-values). Shaded colours indicate gene variants present in both lists.

Rank	Scar Height (SH)						Scar Pliability (SP)					
	SNP[1]	**Gene[2]**	**Distance to gene (base pairs)**	**Exonic function**	**β co-efficient (effect allele)**	***P*-value**	**SNP[1]**	**Gene[2]**	**Distance to gene (base pairs)**	**Exonic function**	**B co-efficient (effect allele)**	***P*-value**
1	rs33117	UBE2E2-AS1	394735	intergenic	-0.254(C)	$3.31x10^{-6}$	rs6703306	GALNT2	0	intronic	0.832(G)	$2.65x10^{-6}$
2	rs1460485	KCNIP4	0	intronic	-0.239(A)	$8.62x10^{-6}$	rs10517350	ARAP2	394063	intergenic	0.724(T)	$3.49x10^{-6}$
3	rs12598337	ATF7IP2	39108	intergenic	-0.418(G)	$2.38x10^{-5}$	rs7234316	DSG1	22587	intergenic	-2.013(A)	$6.34x10^{-6}$
4	rs7645913	ZNF385D	32431	intergenic	0.272(C)	$2.48x10^{-5}$	rs12598337	ATF7IP2	39108	intergenic	-0.441(G)	$8.36x10^{-6}$
5	rs1112017	SLC24A2	219687	intergenic	0.246(C)	$3.01x10^{-5}$	rs11191514	CNNM2	0	intronic	0.416(T)	$1.74x10^{-5}$
6	rs4121859	LOC100129203	210572	intergenic	0.259(A)	$3.52x10^{-5}$	rs598650	TECTA	0	intronic	-0.268(T)	$2.26x10^{-5}$
7	rs978239	UBE2E2	395083	intergenic	0.232(G)	$4.14x10^{-5}$	rs16953087	VPS53	0	UTR3	-0.520(C)	$3.40x10^{-5}$
8	rs782847	LOC646241	22428	intergenic	0.301(C)	$4.33x10^{-5}$	rs11191447	AS3MT, BORCS7-ASMT	0	ncRNA_ intronic	0.403(T)	$3.43x10^{-5}$
9	rs873913	TRIM9	0	intronic	-0.300(G)	$4.91x10^{-5}$	rs11191454	AS3MT, BORCS7-ASMT	0	ncRNA_ intronic	0.404(G)	$3.47x10^{-5}$
10	rs7680585	LINC00499	184812	intergenic	-0.335(A)	$5.05x10^{-5}$	rs873913	TRIM9	0	intronic	-0.305(G)	$3.70x10^{-5}$
11	rs1465405	HTR4	82112	intergenic	-0.250(G)	$5.68x10^{-5}$	rs12472967	EPHA4	340528	intergenic	2.373(T)	$3.73x10^{-5}$
12	rs909017	UBE2E2-AS1	431724	intergenic	0.235(T)	$6.10x10^{-5}$	rs11191548	NT5C2	1596	intergenic	0.400(C)	$3.81x10^{-5}$

13	rs34429154	LOC284661	108376	intergenic	-0.220(C)	$6.67x10^{-5}$	rs11191580	NT5C2	0	intronic	0.400(C)	$3.81x10^{-5}$
14	rs2336046	ZNF385D	24928	intergenic	0.280(C)	$7.59x10^{-5}$	rs11191593	NT5C2	0	intronic	0.400(C)	$3.81x10^{-5}$
15	rs1547918	CDK8	52998	intergenic	0.229(C)	$7.60x10^{-5}$	rs7032556	GAS1	90623	intergenic	-0.624(A)	$4.05x10^{-5}$
16	rs522737	*GRIK2*	*1104043*	intergenic	0.280(G)	$7.66x10^{-5}$	rs12413409	CNNM2	0	intronic	0.399(A)	$4.19x10^{-5}$
17	rs898586	ITGA11	0	intronic	0.313(A)	$7.93x10^{-5}$	rs1065341	CCL5	0	UTR3	0.496(G)	$4.39x10^{-5}$
18	rs55645458	DRC7	0	synonymous	0.489(A)	$9.00x10^{-5}$	rs8081803	PAFAH1B1	0	intronic	0.240(C)	$4.70x10^{-5}$
19	rs10500388	CPPED1	38176	intergenic	-0.279(T)	$9.35x10^{-5}$	rs10905304	GATA3	91934	intergenic	-0.276(A)	$4.80x10^{-5}$
20	rs1792137	TENM4	0	intronic	0.225(G)	$9.86x10^{-5}$	rs898586	ITGA11	0	intronic	0.322(A)	$4.88x10^{-5}$
21	rs10904588	LOC101927762	3054	intergenic	0.219(G)	$1.04x10^{-4}$	rs1378006	EPHA4	484685	intergenic	0.242(A)	$5.34x10^{-5}$
22	rs6678459	AJAP1	124677	intergenic	0.244(T)	$1.09x10^{-4}$	rs1547918	CDK8	52998	intergenic	0.233(C)	$5.67x10^{-5}$
23	rs192923495	DHODH	0	synonymous	2.213(T)	$1.22x10^{-4}$	rs508151	RP11-567M16.3	49966	intergenic	-0.218(G)	$5.94x10^{-5}$
24	rs848641	FEZ2	0	intronic	-0.965(A)	$1.27x10^{-4}$	rs2010190	ALDH5A1	0	intronic	0.387(C)	$6.07x10^{-5}$
25	rs16863161	MED12L	0	intronic	0.965(C)	$1.27x10^{-4}$	rs191586330	KDM2B	0	synonymous	-1.207(C)	$6.56x10^{-5}$
26	rs1827593	KCNIP4, LOC105374516	0	ncRNA_ intronic	0.272(G)	$1.27x10^{-4}$	rs10498593	LINC00911	0	intronic	-0.314(T)	$6.57x10^{-5}$
27	rs10517350	ARAP2	394063	intergenic	0.596(T)	$1.40x10^{-4}$	rs6596006	CDC42SE2	24289	intergenic	0.269(T)	$6.68x10^{-5}$
28	rs10741231	MIR378C	79172	intergenic	0.214(T)	$1.43x10^{-4}$	rs1886715	GPR139	0	intronic	0.272(G)	$7.41x10^{-5}$
29	rs2196346	THSD7B	0	intronic	0.207(A)	$1.50x10^{-4}$	rs6544397	LOC388942	664825	intergenic	0.262(C)	$7.65x10^{-5}$
30	rs7956979	TMEM132B	0	intronic	0.222(A)	$1.53x10^{-4}$	rs6893965	FLJ16171	70396	intergenic	0.340(T)	$7.74x10^{-5}$

31	rs11134474	SGCD	551239	intergenic	-0.926(G)	$1.54x10^{-4}$	rs3011271	SNORD141A, SNORD141B	12197	intergenic	-0.270(T)	$7.82x10^{-5}$
32	rs13315591	FAM107A	0	intronic	0.386(C)	$1.56x10^{-4}$	rs4894081	SESTD1	0	intronic	-0.234(G)	$7.95x10^{-5}$
33	rs1816918	SCN2A	0	intronic	0.279(C)	$1.56x10^{-4}$	rs12505296	LOC102723766	0	intronic	-0.258(C)	$7.97x10^{-5}$
34	rs252811	EFNA5	0	intronic	-0.258(C)	$1.60x10^{-4}$	rs35954941	DLGAP5	0	synonymous	-1.251(G)	$8.13x10^{-5}$
35	rs4908736	LOC102724539	81521	intergenic	0.307(G)	$1.60x10^{-4}$	rs9409144	DEC01	0	intronic	-0.210(T)	$8.54x10^{-5}$
36	rs12049330	ATXN7L2	0	intronic	-0.278(G)	$1.61x10^{-4}$	rs4474514	KITLG	0	intronic	0.255(G)	$8.63x10^{-5}$
37	rs347134	CMTM7	0	intronic	-0.217(G)	$1.68x10^{-4}$	rs1000788	KITLG	0	intronic	0.254(G)	$8.65x10^{-5}$
38	rs1573224	SLC24A2	155294	intergenic	0.218(G)	$1.70x10^{-4}$	rs6678459	AJAP1	124677	intergenic	0.247(T)	$8.67x10^{-5}$
39	rs2230808	ABCA1	0	non-synonymous	-0.244(A)	$1.75x10^{-4}$	rs9293732	AP3B1	0	intronic	0.227(T)	$9.14x10^{-5}$
40	rs9293732	AP3B1	0	intronic	0.217(T)	$1.82x10^{-4}$	rs3907470	KITLG	0	intronic	0.252(C)	$9.37x10^{-5}$
41	rs13188076	HTR4	65903	intergenic	-0.238(T)	$1.86x10^{-4}$	rs7743582	C6orf58	24898	intergenic	0.586(C)	$1.00x10^{-4}$
42	rs1101751	PCED1B	0	intronic	0.228(G)	$1.90x10^{-4}$	rs7595014	NRXN1	153588	intergenic	0.227(G)	$1.04x10^{-4}$
43	rs12037569	SORT1	0	intronic	-0.268(T)	$1.93x10^{-4}$	rs7653621	MIR548A3	241380	intergenic	-0.220(T)	$1.05x10^{-4}$
44	rs2731840	EFNA5	0	intronic	-0.243(C)	$1.95x10^{-4}$	rs17252034	LINC00371	8583	intergenic	0.328(C)	$1.05x10^{-4}$
45	rs6732045	HAAO	62454	intergenic	2.623(A)	$1.99x10^{-4}$	rs3782181	KITLG	0	intronic	0.251(C)	$1.12x10^{-4}$
46	rs1364795	NAV2	0	intronic	0.260(C)	$2.05x10^{-4}$	rs161799	PARK7	6154	intergenic	-0.234(C)	$1.16x10^{-4}$
47	rs3736493	ITGA11	0	non-synonymous	0.261(C)	$2.10x10^{-4}$	rs7298378	PTPRR	0	intronic	-0.338(G)	$1.17x10^{-4}$

48	rs61818256	PKP1	0	synonymous	0.720(T)	$2.23x10^{-4}$	rs16863161	MED12L	0	intronic	0.958(C)	$1.42x10^{-4}$
49	rs1431494	MED12L	0	intronic	0.929(G)	$2.27x10^{-4}$	rs2731840	EFNA5	0	intronic	-0.246(C)	$1.43x10^{-4}$
50	rs6142443	PHF20	0	intronic	-0.236(A)	$2.30x10^{-4}$	rs4269843	CH25H	21478	intergenic	-0.284(A)	$1.45x10^{-4}$

1. Human reference genome version GRCh37 (hg19).
2. Gene nearest to SNP.

Table 3. *P*-values for genetic variants reported to be associated with HTS in previous studies.

Gene	Reference	SNP/gene variant	Sample	Type of study	Outcome measure	Effect on scar component	*P*-value	*P*-value in current study [threshold $P<1.7x10^{-7}$]
TGFB1 [Transforming growth factor beta 1]	[15]	rs8110090	202 adults with surgical wound excision	Candidate SNP approach	Total VSS score (omitting pigmentation)	Increased risk of poor scar outcome	*Q*=0.006 (FDR adjusted *P*-value)	All TGFB1 SNP *P* >0.01 for height and pliability [rs8110090 not included in HumanCoreExome Beadchip microarray]
HLA-DR [human leukocyte antigen - antigen D related]	[23]	HLA-DRB1*16	128 adults (19 with HTS after burn injury; 109 healthy community controls)	Candidate gene approach (HLA class II allogenotypes)	HTS (clinical diagnosis)	Increased risk of HTS (relative risk 12.25)	$P=1.45\times10^{-4}$ (corrected for multiple testing)	Height: NS (β=0.063; *P*=0.269) Pliability: NS (β=0.076; *P*=0.185) (based on rs6923504 - partial tag SNP for HLA-DRB1*16 in Europeans included in HumanCoreExome Beadchip microarray [58])
MC1R [melanocortin 1 receptor]	[11]	rs885479	413 adults with burn injury (subset of subjects in Sood et al. 2015 [17])	Candidate SNP approach (8 SNPs)	Severe HTS (dichotomous variable: total VSS score ≤7 vs. >7)	Severe HTS: Adjusted prevalence ratio=1.35	*P*<0.001 (threshold *P*<0.01)	All MC1R SNP *P* >0.01 for height and pliability [rs885479 and the other 7 SNPs tested not included in HumanCoreExome Beadchip microarray]
CSMD1 [CUB and Sushi multiple domains 1]	[17]	rs11136645	538 adults with burn injury	GWAS	Scar height (four categories treated as continuous	Height: β=−0.23	$P=7.9\times10^{-8}$ (threshold $P<2\times10^{-7}$)	Scar height NS (β=−0.013; *P*=0.8066)

					variable in linear regression)			
PTPN5 [protein tyrosine phosphatase, non-receptor type 5]	[14]	rs56234898	538 adults with burn injury (same subjects as Sood et al. 2015 [17])	Candidate gene pathway approach – subset of GWAS data (mitogen-activated protein kinase [MAPK] pathways: 4,912 SNPs)	All four VSS variables tested simultaneously in a joint, inverted regression model	Height: β=−0.002 Pliability: β=−0.007 Pigmentation: β=0.206 Vascularity: β=−0.006	$P=1.3\times10^{-6}$ (threshold $P<2\times10^{-5}$)	Height: NS (β=0.351; $P=0.141$) Pliability: NS (β=0.402; $P=0.091$) Pigmentation: nd Vascularity: nd

FDR = false discovery rate; nd = not done; NS = not significant.

Table 4. Enriched 'biological process' gene ontology (GO) terms for scar height and pliability (*P*<1.68E-06; Bonferroni correction for multiple 'Biological process' gene ontology (GO) terms).

'Biological process' gene ontology (GO) term	Gene Ontology (GO) ID	# of Entities	Overlap	Percent Overlap	*P*-value	Jaccard similarity
Scar Height (SH)						
Axon guidance	0007411;0008040	385	82	21	$2.95x10^{-17}$	0.028
Multicellular organismal development	0007275	1171	169	14	$1.50x10^{-15}$	0.047
Cell differentiation	0030154	849	132	15	$8.52x10^{-15}$	0.040
Nervous system development	0007399	523	93	17	$3.42x10^{-14}$	0.031
Synaptic transmission	0007268	472	84	17	$5.78x10^{-13}$	0.028
Cell adhesion	0007155	616	98	15	$7.07x10^{-12}$	0.032
Positive regulation of transcription from RNA polymerase II promoter	0045944;0045817;0010552	1041	139	13	$1.65x10^{-10}$	0.040
Regulation of ion transmembrane transport	0034765	191	42	21	$5.73x10^{-10}$	0.015
Synaptic transmission, glutamatergic	0035249	43	18	41	$9.10x10^{-10}$	0.007
Extracellular matrix organisation	0030198	329	57	17	$2.79x10^{-7}$	0.019
Regulation of membrane potential	42391	91	24	26	$4.92x10^{-7}$	0.008
Adherens junction organization	34332	40	15	37	$5.08x10^{-7}$	0.005
Transport	0006810;0015460;0015457	1853	219	11	$5.64x10^{-7}$	0.050
Ionotropic glutamate receptor signaling pathway	35235	27	12	44	$8.19x10^{-7}$	0.004
Potassium ion transmembrane transport	71805	134	30	22	$9.33x10^{-7}$	0.010
Potassium ion transport	0015458;0006813	136	30	22	$1.30x10^{-6}$	0.010
Skeletal system morphogenesis	48705	59	18	30	$1.31x10^{-6}$	0.006
Cell junction assembly	34329	77	21	27	$1.38x10^{-6}$	0.007
Cell-cell junction organization	45216	71	20	28	$1.41x10^{-6}$	0.007
Scar Pliability (SP)						
Cell adhesion	0007155	616	116	18	$1.68x10^{-20}$	0.039
Nervous system development	0007399	523	98	18	$2.41x10^{-17}$	0.033

Multicellular organismal development	0007275	1171	153	13	8.20×10^{-12}	0.043
Synaptic transmission	0007268	472	79	16	1.34×10^{-11}	0.027
Homophilic cell adhesion via plasma membrane adhesion molecules	0007156	161	39	24	4.31×10^{-11}	0.015
Positive regulation of transcription from RNA polymerase II promoter	0045944;0045817;0010552	1041	137	13	6.59×10^{-11}	0.040
Axon guidance	0007411;0008040	385	66	17	2.30×10^{-10}	0.023
Cell-cell junction organization	0045216	71	23	32	9.62×10^{-10}	0.009
Cell junction assembly	0034329	77	23	29	5.68×10^{-9}	0.009
Single organismal cell-cell adhesion	0016337	145	33	22	7.15×10^{-9}	0.012
Regulation of membrane potential	0042493;0017035	91	25	27	8.43×10^{-9}	0.010
Signal transduction	0042493;0017035	1843	207	11	1.199×10^{-8}	0.050
Ion transport	0042493;0017035	627	87	13	1.97×10^{-8}	0.029
Cell differentiation	0042493;0017035	849	107	12	8.49×10^{-8}	0.033
Adherens junction organization	0042493;0017035	40	15	37	8.69×10^{-8}	0.006
Glutamate receptor signaling pathway	0042493;0017035	14	9	64	1.06×10^{-7}	0.004
Negative regulation of cell proliferation	0042493;0017035	471	68	14	1.57×10^{-7}	0.024
Intracellular signal transduction	0042493;0017035	519	73	14	1.59×10^{-7}	0.025
Negative regulation of transcription from RNA polymerase II promoter	0042493;0017035	799	101	12	1.70×10^{-7}	0.032
Negative regulation of cell proliferation	0042493;0017035	471	68	14	3.83×10^{-7}	0.024
Transmembrane transport	0042493;0017035	805	100	12	4.46×10^{-7}	0.031
Sensory perception of sound	0042493;0017035	157	31	19	6.04×10^{-7}	0.012
Regulation of ion transmembrane transport	0042493;0017035	191	35	18	7.58×10^{-7}	0.013
Locomotory behavior	0042493;0017035	108	24	22	1.23×10^{-6}	0.009
Ion transmembrane transport	0042493;0017035	291	46	15	1.29×10^{-6}	0.017
Response to drug	0042493;0017035	509	69	13	1.34×10^{-6}	0.024

COMPETING INTERESTS

The authors have no competing financial interests to declare.

Supplementary Figure S1. Patient treatment algorithm: optimal clinical treatment pathway for patients with burn injury in the care of (a) Burns Service of Western Australia; (b) Alder Hey Children's Hospital, Liverpool, UK.

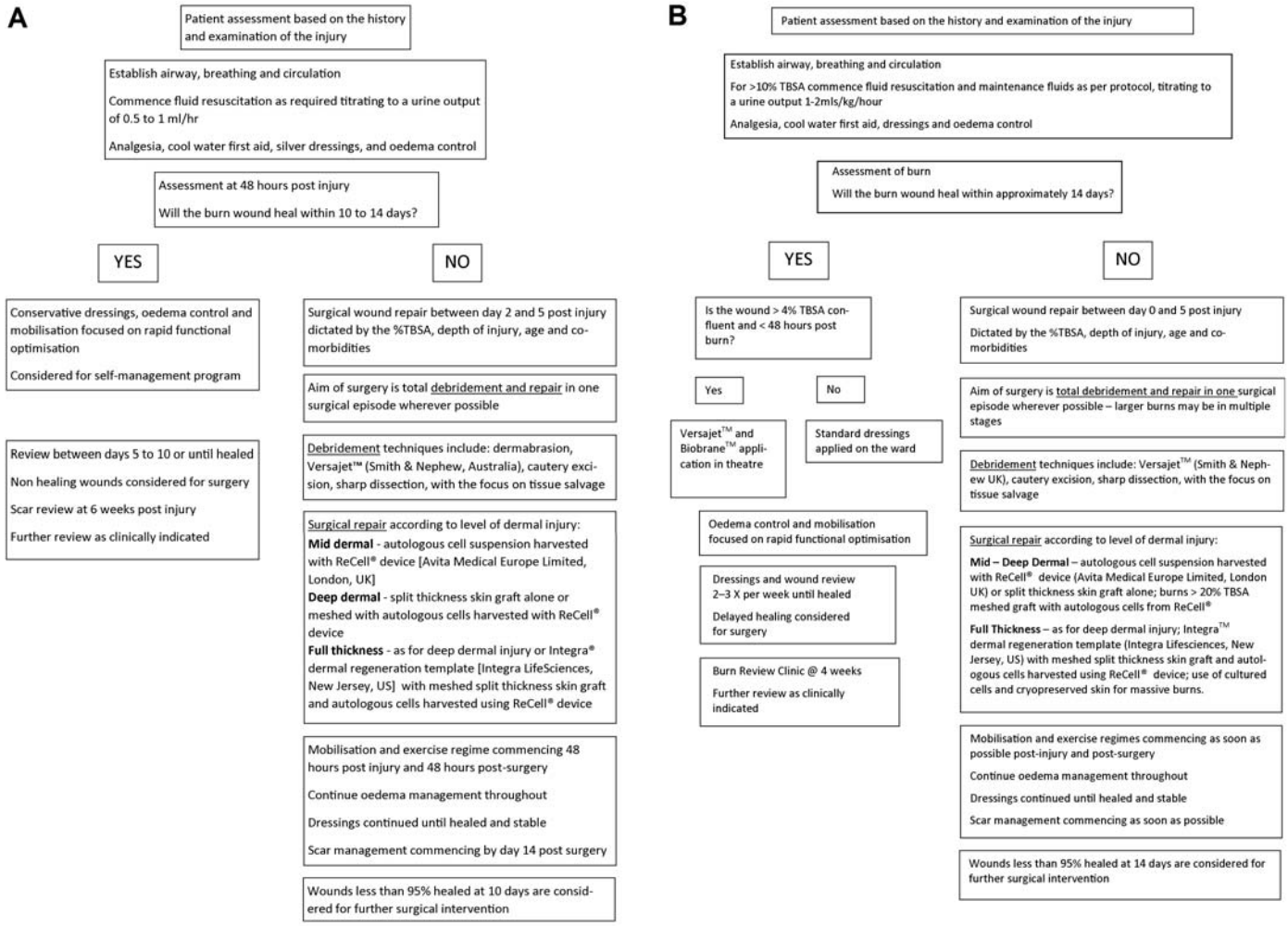

Supplementary Figure S2. Sample size required to achieve 80% statistical power given a range of effect sizes and minor allele frequencies. Effect sizes are presented in standard deviation (SD) units. Assumptions: An additive model with statistical significance of 5.0×10^{-8}. MAF: Minor allele frequency; SD: standard deviation. Power calculation performed in Quanto (Gauderman WJ, Morrison JM. QUANTO 1.1: A computer program for power and sample size calculations for genetic epidemiology studies, http://hydra.usc.edu/gxe, 2006.

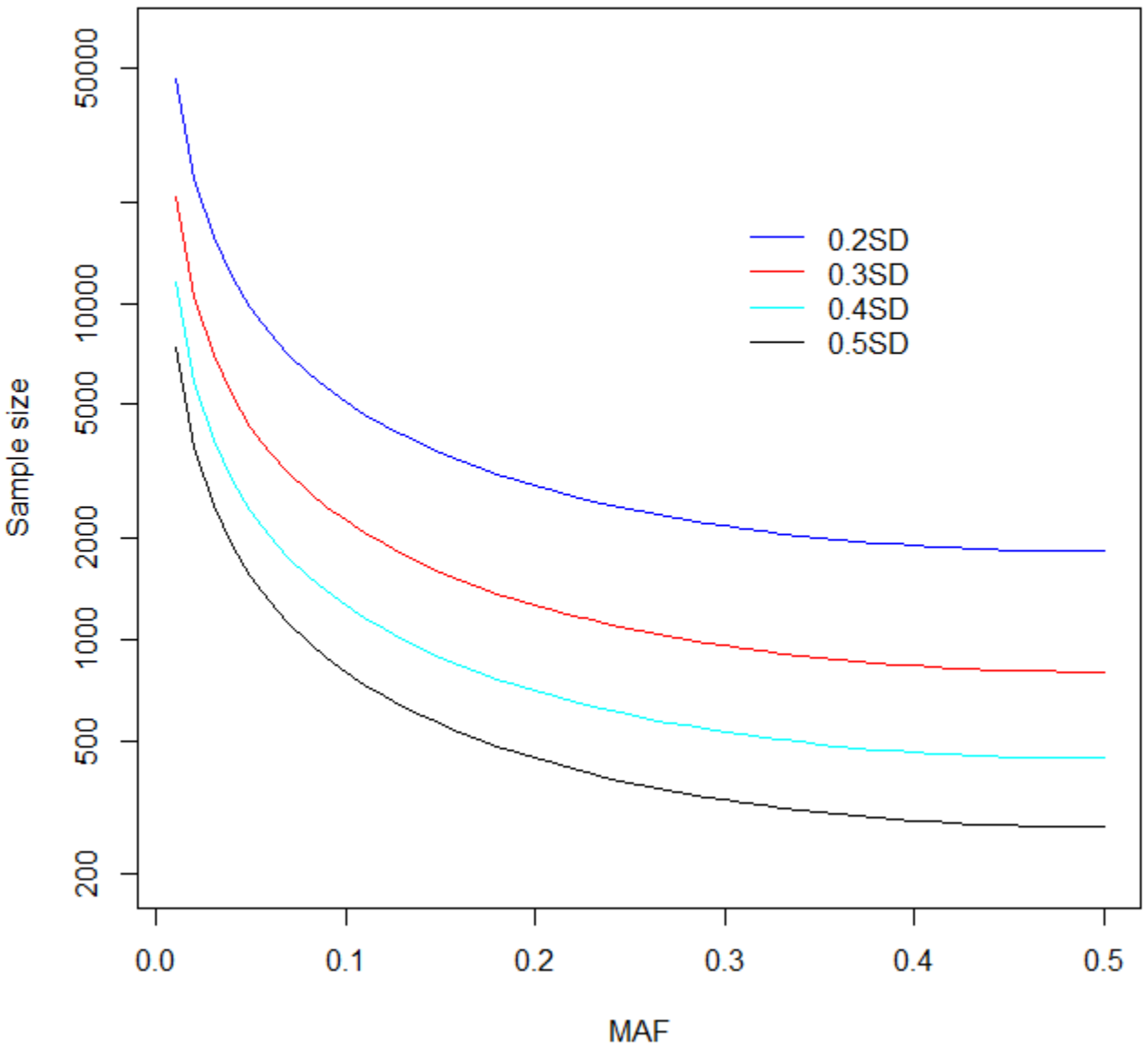

Supplementary Figure S3. Cross-tab plots showing the relationship between (a) scar height (SH) and scar pliability (SP) scores (r=0.90); (b) SH and total mVSS scores (r=0.91); (c) SP and total mVSS scores (r=0.91); (d) [SH+SP] and total mVSS scores (r=0.94). Plot (e) shows the relationship between the linear model residuals for SH and SP after adjustment by age, sex, number of surgeries, % body surface area and the 1st principal component. Residuals presented have been inverse-rank normalised.

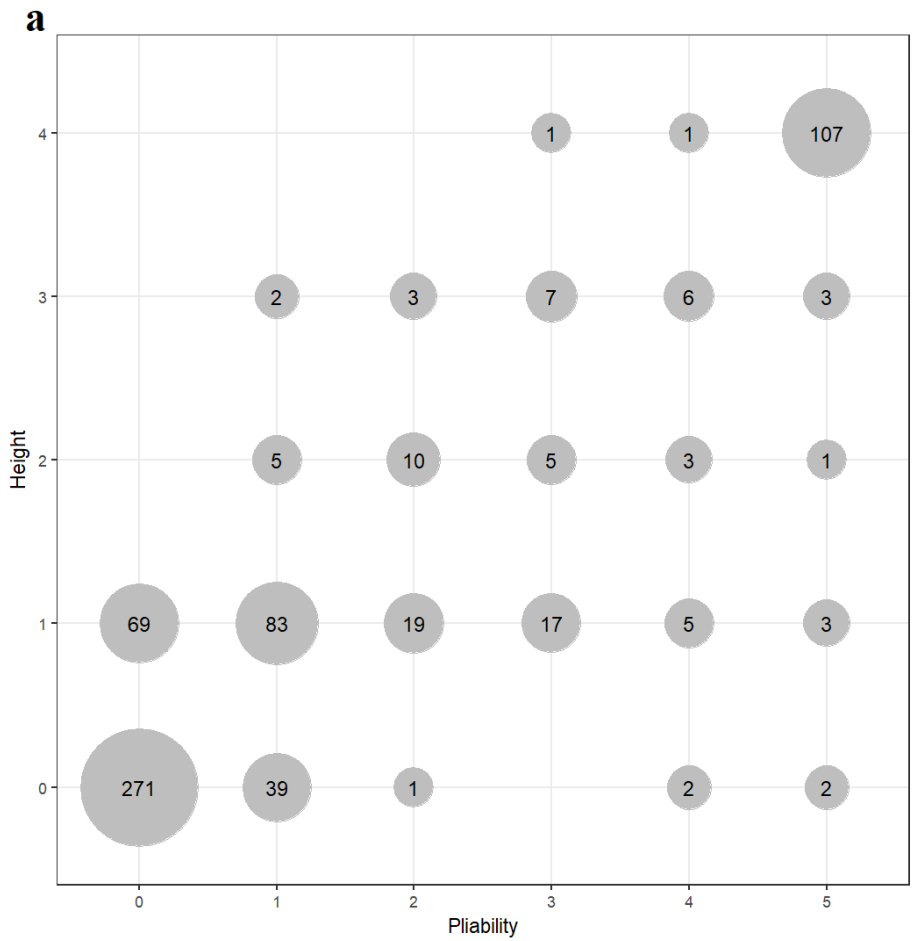

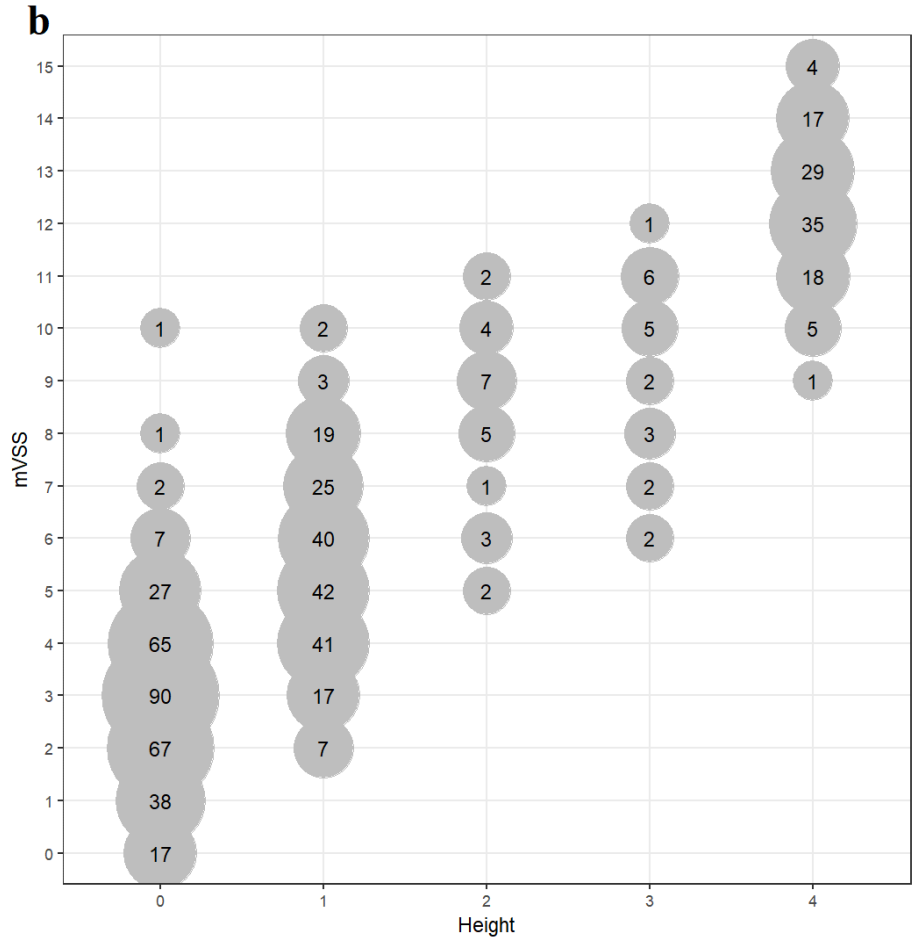

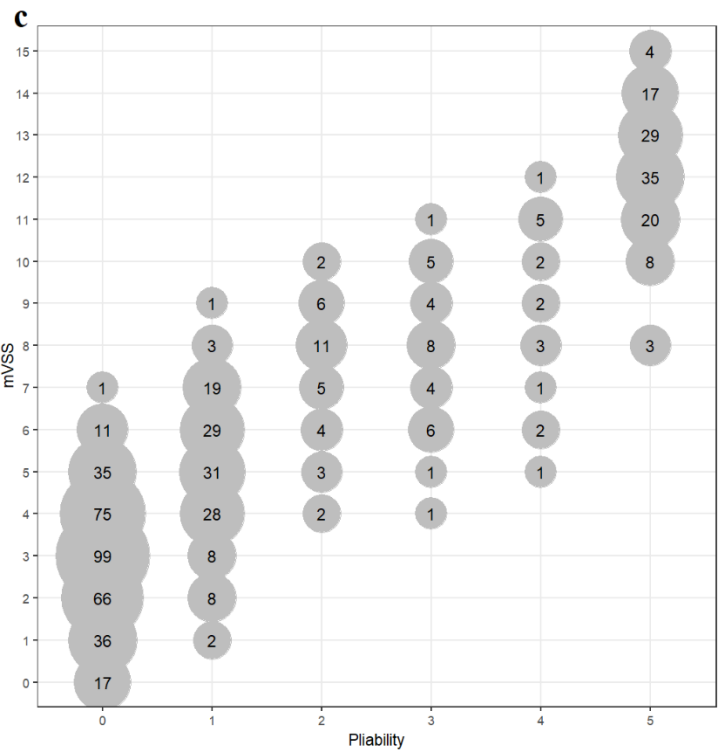
c
mVSS
Pliability
0 1 2 3 4 5
0 1 2 3 4 5 6 7 8 9 10 11 12 13 14 15
1 11 35 75 99 66 36 17
1 3 19 29 31 28 8 8 2
2 6 11 5 4 3 2
1 5 4 8 4 6 1 1
1 5 2 2 3 1 2 1
4 17 29 35 20 8 3

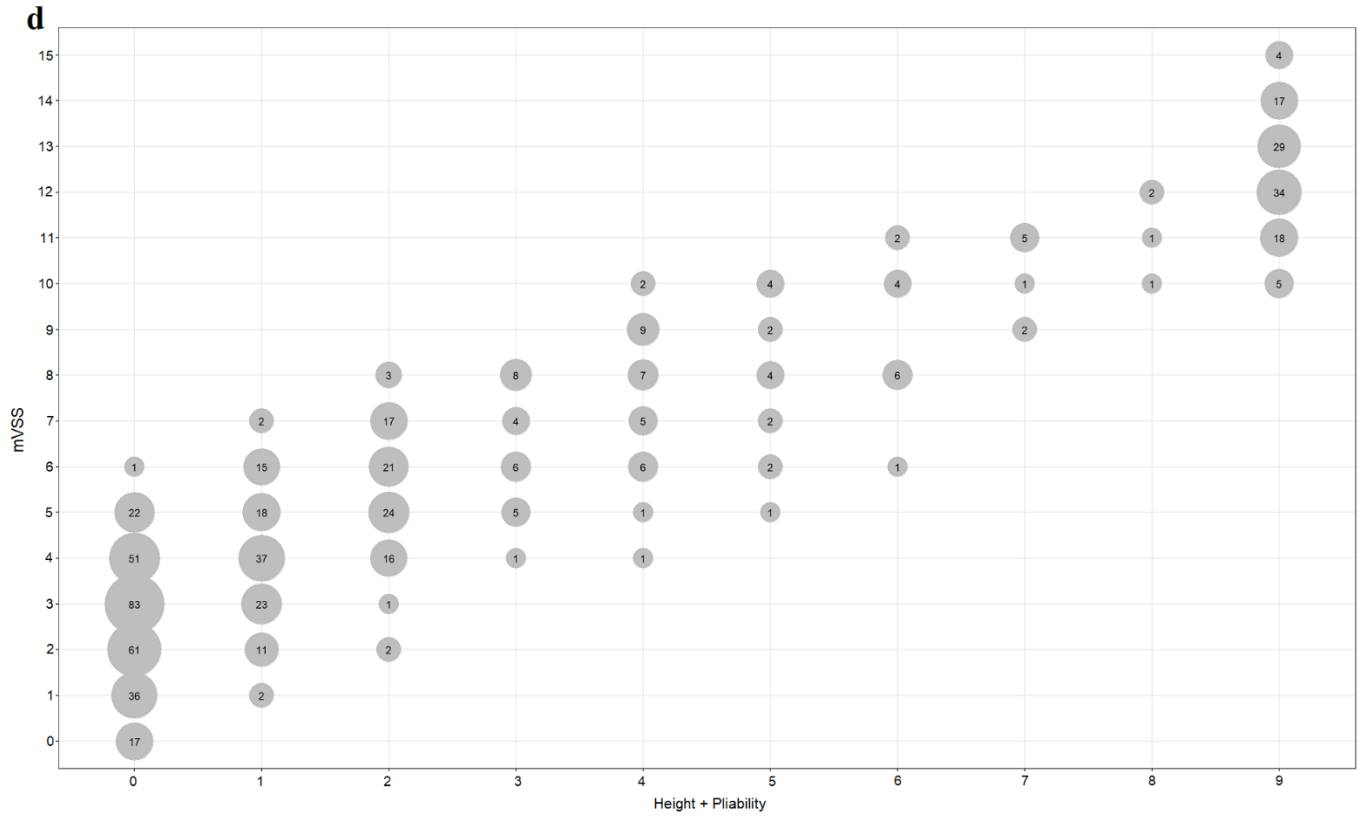
d
mVSS
Height + Pliability
0 1 2 3 4 5 6 7 8 9
0 1 2 3 4 5 6 7 8 9 10 11 12 13 14 15
1 22 51 83 61 36 17
2 15 18 37 23 11 2
3 17 21 24 16 1 2
8 4 6 5 1
2 9 7 5 6 1 1
4 2 4 2 2 1
2 4 6 1
5 1 2
2 1 1
4 17 29 34 18 5

e

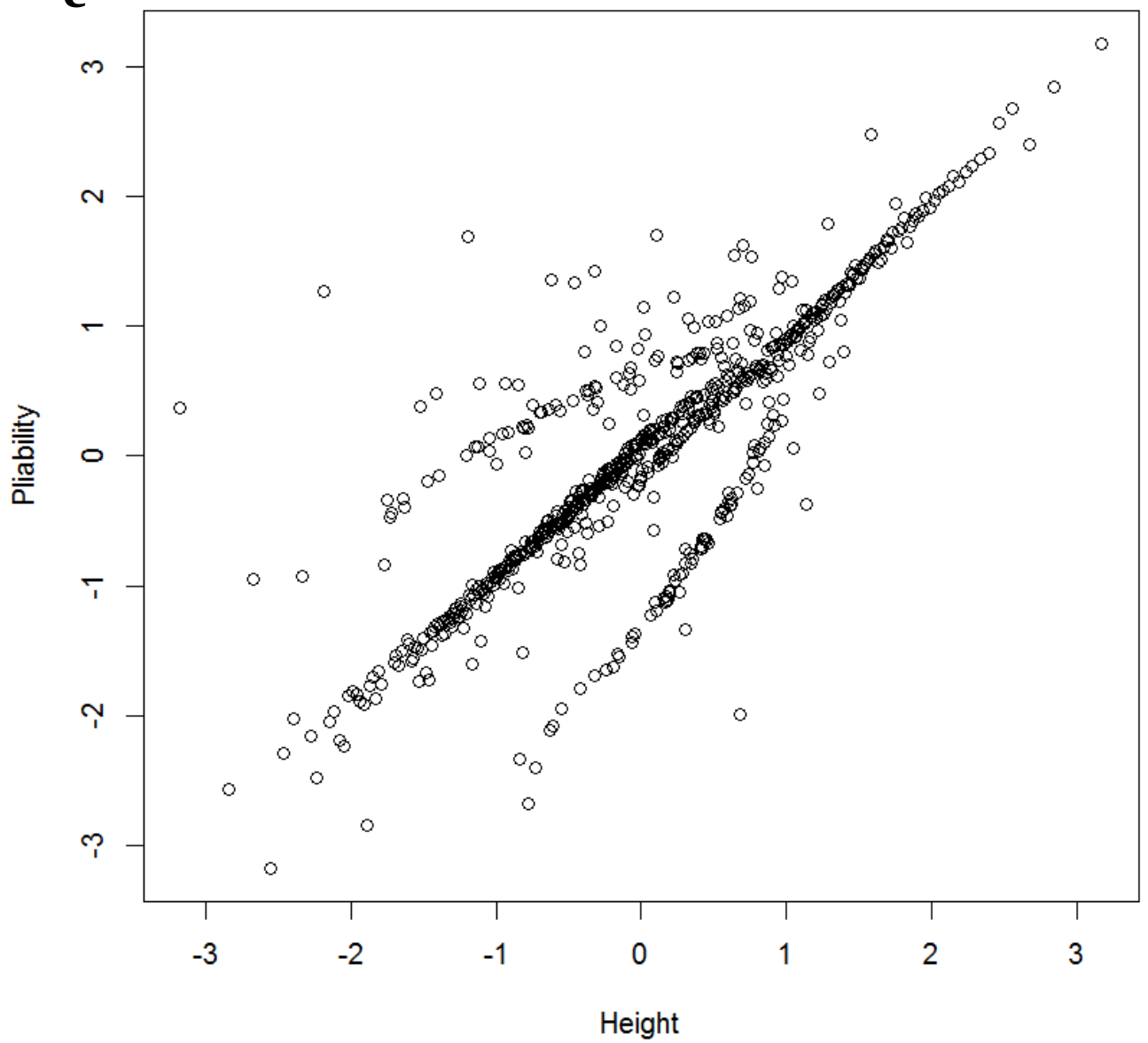

Supplementary Figure S4. QQ (quantile-quantile) plots of the expected distribution of association test statistics (X-axis) across all SNPs compared to the observed values (Y-axis): (A) scar height (SH); (B) scar pliability (SP). The observed distribution of *P*-values for the 298,150 SNPs exhibited minimal deviation from the expected distributions for both outcomes.

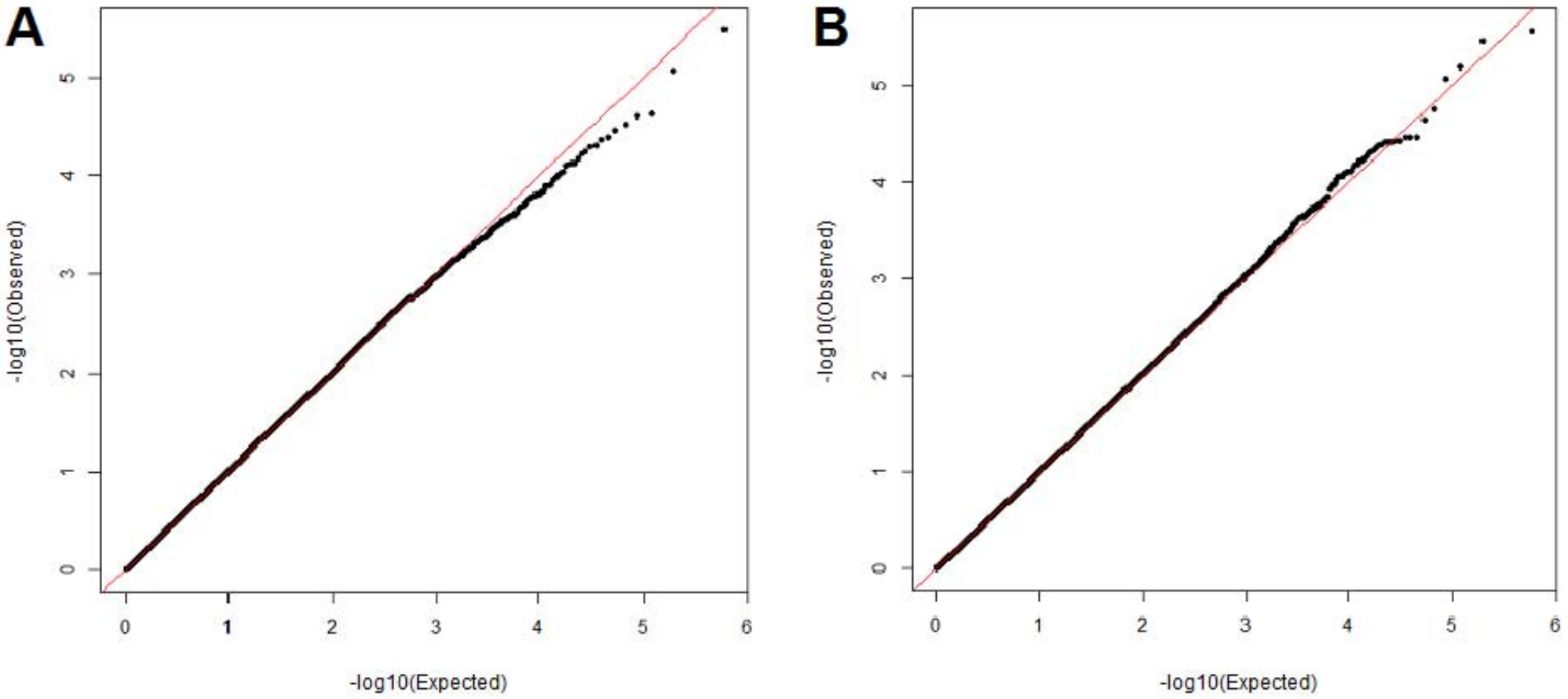

Supplementary Table S1. The association between patient characteristics and scar height and pliability.

	Scar Height			Scar Pliability		
Variable	**β coefficient**	**Standard Error**	***P*-value**	**β coefficient**	**Standard Error**	***P*-value**
Age (years)	-0.015	0.002	1.17E-10	-0.018	0.003	5.04E-09
Male sex	-0.302	0.099	0.00243	-0.348	0.132	0.00851
TBSA (%)	0.044	0.005	< 2E-16	0.055	0.006	< 2E-16
Number of surgeries	0.677	0.089	7.78E-14	0.885	0.118	1.85E-13

Supplementary Table S4. Enriched '*biological process'* gene ontology (GO) terms associated with scar height (SH) (*P*<1.68E-06; Bonferroni correction for multiple pathways). (Gene regions imported into Pathway Studio® were identified as those with at least two SNP sites and *P*-value <0.01).

Name	GO ID	# of Entities	Overlap	Percent Overlap	Overlapping Entities	*P*-value	Jaccard similarity
axon guidance	0007411; 0008040	385	82	21	EPHA4;GLI2;RPS6KA2;DCC;NRP1;CLASP2; KRAS;LMTK2;EFNA5;AGRN;SRGAP2; GRIN2B;EPHA7;SEMA4F;GATA3;SLIT2; SLIT3;KCNQ3;NRXN3;CACNB2;NGEF; CNTN6;SEMA3A;MMP2;RPS6KA4; ABLIM2;EFNB2;RAC2;SCN5A;NTN4;TNR; VAV3;FYN;CNTN4;ISPD;COL5A2;COL6A3; MATN2;ETV1;LAMB1;GBX2;COL9A1; B3GNT2;ATOH1;TRPC7;ST8SIA2;TBR1; COL4A1;RGMA;SEMA5A;AP2B1;LMX1A; CDH4;MYH11;LHX2;SEMA3E;COL3A1; CHL1;KIF4B;ARHGEF28;RELN;NRXN1; UNC5D;BMP7;ANK2;RGMB;UNC5C; TENM2;EPHB3;TIAM1;UNC5A;SOS1; GAS1;PRNP;ALCAM;GLI3;PLXNA2;PRKCQ; OR8A1;DPYSL2;COL2A1;SRGAP1	2.95E-17	0.028462
multicellular organismal development	0007275	1171	169	14	CCBE1;DDX4;EPHA4;DAZL;TNFRSF11A; NANOS2;DCC;DNER;NRP1;SPRY4;TDRD6; BMP4;SPRED1;SPRED2;SFRP2;QKI; DPY19L2;ERBB4;EMX2;EDIL3;PIWIL3; PIWIL2;MKX;NTRK2;PIWIL1;MAEL;FLT1; FOXA2;TSHZ2;LRIG3;KIAA1217;FGF1;HLF; TMEM2;FRAT2;SHISA3;TCL1A;CSPG4; MAK;GOLGA3;EFNA5;AGRN;KIF26B;	1.51E-15	0.047207

					SLC2A14;TP63;SPATA16;PAX5;SLC22A16; NOTCH4;GDF6;STRBP;BST1;PAFAH1B1; OSTN;PSME4;CATSPERD;EPHA7; CATSPER3;DIAPH2;NKX61;NAV1;MITF; TBC1D32;ADCYAP1R1;DSPP;SEMA4F; GFI1B;JARID2;SLIT2;SFRP1;SLIT3;PDGFRA ;NGEF;PDGFD;SEMA3A;HOXD9;RYBP; NSD1;EFNB2;PHACTR4;DACH1;MYF6; ZBTB18;HTATIP2;SORT1;BIN1;FYN; CTNNA2;NTNG1;DISP1;ATOH1;CUX1; CHST2;DAB1;SEMA5A;EMP1;LMX1A; IFRD1;SEMA3E;SOX6;FAT3;TCF4;CRX; OLIG2;TBX3;LBX1;OLFM1;FARP1;PAX3; CHL1;RELN;EGFL6;EYA4;WLS;TAL1; UNC5D;BMP7;TMEM100;LRP5;FZD6; UNC5C;PIM1;PDPN;KIF2A;NEUROD6; CCHCR1;ZNF521;NEUROD2;NUS1; SEMA3D;LCLAT1;HOXC6;EPHB3;PBXIP1; MYT1L;UNC5A;ARHGAP24;MDGA1;HELT; TENM4;G2E3;PAX1;GAS7;HOXC4; ADRA1D;TBX4;FGF3;GSC;NEUROD1;GLI3; EID2;TLE1;TWSG1;CHRD;VWC2L;HOXD8; DACT1;CASZ1;PLXNA2;DBX1;EBF2;ZFP64; PBX1;PITX1;SPRY2;INSC;DPYSL2; EDARADD;ZFP57		
cell differentiation	0030154	849	132	15	GLI2;NANOS2;DNER;NRP1;TDRD6;BMP4; KIT;SFRP2;QKI;DPY19L2;PIWIL3;MEIG1; LRRK2;HFM1;KIAA0430;PIWIL2;NTRK2; PIWIL1;MAEL;FLT1;M1AP;FGF1;CSPG4; MAK;GOLGA3;SPATA31D1;EFNA5;AGRN;	8.52E-15	0.040061

					NR0B1;DRC7;SLC2A14;TP63;SPATA16; PAX5;SLC22A16;NOTCH4;GALNTL5; STRBP;PAFAH1B1;OSTN;PSME4;KLF4; CATSPERD;CATSPER3;FER;PARD3; NKX6-1;NAV1;MITF;ETV2;ADCYAP1R1; SEMA4F;TFAP2C;JARID2;SLIT2;SFRP1; SLIT3;ETS1;NGEF;FLI1;SEMA3A;STX2; PRKD1;EFNB2;HCK;MYF6;HTATIP2; SORT1;BIN1;FYN;FLNB;CTNNA2;SRPK2; NTNG1;ETV1;ATOH1;DAB1;TEC; SEMA5A;IFRD1;SEMA3E;CTBP2;NELL1; TCF4;CRX;LBX1;UBE2V1;CHL1; ARHGEF28;EGFL6;TAL1;BATF;BMP7; TMEM100;OSR1;KIF2A;NFATC4; NEUROD6;CCHCR1;SRRM4;ZFPM2; ZNF521;NEUROD2;NUS1;SEMA3D;ELF4; SSPO;CBX2;TRAPPC9;ZNF431;PBXIP1; MYT1L;ETV6;THSD7A;ARHGAP24; MDGA1;ABHD5;HELT;TENM4;TENM3; PLAGL1;GAS7;FGF3;NEUROD1; PRDM16;EID2;TWSG1;PBX1;RXFP1;INSC; DPYSL2;EDARADD		
nervous system development	0007399	523	93	17	EPHA4;NRP1;EPM2A;GFRA2;FOS;DPF3; ERBB4;DOK5;NTRK2;LMTK2;EFNA5; SRGAP2;SPG7;PAX5;PAFAH1B1;EPHA7; NAV1;SEMA4F;GATA3;SLIT2;SLIT3; NOVA1;ADCYAP1;NGEF;CNTN3;NRSN1; SRGAP2B;SEMA3A;HDAC4;HDAC9;PRKD1 ;EFNB2;GRIK1;PHACTR4;NLGN1;MYO1B; CRIM1;THBS4;TNR;PEX2;CNTN4;MYLIP;	3.42E-14	0.030918

					NRN1;NTNG1;GBX2;ATOH1;ST8SIA2; ELAVL4;BTBD3;GRIP1;DAB1;RAPGEF5; GMFB;SEMA5A;DSCAM;LHX2;SEMA3E; NELL1;PCSK2;TCF4;CYB5D2;CRX;OLIG2; LBX1;OLFM1;LSAMP;FUT9;SPOCK1;PAX3; CHL1;DYRK1A;ANK2;PDPN;KIF2A; NEUROD6;SRRM4;NEUROD2;SEMA3D; SSPO;CHRM3;EPHB3;SCN2A;MYT1L; BRSK2;MDGA1;HELT;GAS7;MAGI2; NEUROD1;NAV2;DACT1;INSC;DPYSL2		
synaptic transmission	0007268	472	84	17	KCNN4;ACTN2;RPS6KA2;OPRM1;KCNH8; KCNH1;GABRG3;GRM4;SSTR4;GRM5; AGRN;CDH8;GRIK2;GRIN2B;NPFFR2; PAFAH1B1;GPR149;DRD1;DLGAP1; KCNQ3;KCNQ5;KCNMA1;KCNA4;KCNG2; KCNK9;NOVA1;NRXN3;KCNAB1;KCNJ6; SLC22A2;CHRNA9;KCNV1;GAD1;HCN1; GABRB1;KCNC4;KCNF1;KCNA3;MBP; ALDH5A1;SV2C;SLC1A3;KCNA6;CACNB2; CLSTN2;PPFIA2;NPTX2;KCNS3;ABAT; GRIK1;GRIN2A;GRIA4;GRIK4;CACNG3; KCNJ3;KCND2;SYT1;RIMS1;GRIP1;AP2B1; UNC13A;PDE7B;GRM8;GRIA1;NRXN1; GABRB3;ADCY8;CAMK2A;GPR139;GRM3; ADCY1;GRIK3;CHRM3;GABRD;GABBR2; HTR4;GRM7;NMBR;GALR1;UNC13C; NPY2R;HRH1;PRKCB;GRIA2	5.78E-13	0.028321
cell adhesion	0007155	616	98	15	EPHA4;ACTN2;KITLG;EDIL3;CDH2; TSPAN5;CDH3;SPG7;CDH5;CDH8; AMICA1;MAGI1;CD2;EMB;FER;SVEP1;	7.07E-12	0.031654

					TPBG;SDK1;LPP;CDH20;DSG1;PCDH10; AJAP1;HAS2;CLSTN2;CNTN6;CNTN3; COL16A1;B4GALT1;DSC3;IGSF11;OLR1; EFNB2;PARVA;HCK;NLGN1;PODXL2; SORBS2;FAT1;PCDH15;THBS4;TNR;DSG3; CNTNAP4;COL6A5;COL6A6;LAMC2; CNTN4;TLN2;CDH23;CTNNA2;COL6A3; LEF1;LAMB1;ITGA11;CDH11;NUAK1; SEMA5A;SCARB1;CDH4;DSCAM;FAT3; GRHL2;LSAMP;ARHGAP5;CD47;SPOCK1; WISP3;CHL1;RELN;NRXN1;EGFL6;CDH13; NTM;CDH12;CADM2;CDH6;CDH9;CDH7; NEDD9;PTPRT;PTPRM;RGMB;PDPN;SSPO ;TENM2;PRKCE;CCR8;TENM3;THBS1; MPZL2;ALCAM;CDH1;LGALS3BP;CNTN5; CNTNAP5;ITGA6;LPXN		
positive regulation of transcription from RNA polymerase II promoter	0045944; 0045817; 0010552	1041	139	13	TRAF6;BARX2;HDGFL1;CREB5;GLI2;TLR3; IL17F;NFATC2IP;BMP4;SFRP2;FOS; TFAP2A;ATXN1;TLR2;SLC11A1;MKX;IL6; DICER1;FOXA2;RBPJ;FGF1;SLC40A1; BLOC1S2;AGRN;BCAS3;TP63;CSRNP1; PAX5;PARK2;GDF2;KLF4; NKX6-1;MITF;ETV2;HMGA1;HSF2; TFAP2C;THRB;NCOA2;GATA3;RUNX1; KPNA6;ADCYAP1;ADRB2;ETS1;FLI1; HDGF;MAML2;NCOA3;PARK7;RPS6KA4; PPARGC1A;HOXD9;HDAC4;TBL1XR1; PRKD1;ABLIM2;DAXX;MYF6;TAF2;DHX36; TCEA1;PIK3R1;NR5A2;LEF1;ETV1; MAP3K1;ATOH1;TBR1;RORA;CUX1;MAF;	1.66E-10	0.039943

					IFRD1;SMAD3;LPIN3;LHX2;CSRNP3;SOX6; FOXF2;CTBP2;TCF4;CRX;NPAS2;SOX5; PAX3;MCF2L;SMAD7;KLF5;CDH13;TAL1; IL4;CDK8;BATF;BMP7;FGFR2;YAP1;LRP5; E2F4;E2F7;NFATC1;GATA5;PKD2;OSR1; AHRR;NFATC4;NEUROD6;LDB2;ZFPM2; NEUROD2;ELF4;NRF1;MYT1L;ETV6; PRPF6;PPARG;HELT;WWOX;GLIS3;PBX2;P AX1;PLAGL1;RARB;NEUROD1;GLI3;FOSB; RUNX2;JADE1;HOXD8;GALR1;LMO4; EBF2;PBX1;PITX1;LPIN1;SSBP3;ZFAT; ITGA6;MKL1;BSX		
regulation of ion transmembrane transport	0034765	191	42	21	TPCN2;KCNH8;KCNH1;TRPM4;KCNE2; KCNT2;KCNE3;KCNK12;KCNIP4; CACNA2D3;CACNA2D1;CATSPER3; KCNQ3;KCNQ5;KCNMA1;KCNA4;KCNG2; KCNK9;KCNAB1;KCNJ6;KCNV1;HCN1; KCNC4;KCNF1;KCNA3;KCNA6;CACNB2; KCNS3;GRIK1;GRIN2A;CACNG3;SCN5A; CLCN1;KCNJ3;KCND2;NEDD4L;CLIC5; NEDD4;NCS1;SCN2A;CNGB3;GRM7	5.74E-10	0.015402
synaptic transmission, glutamatergic	0035249	43	18	41	GRM4;CDH8;PARK2;GRIK2;GRIN2B; ADRB2;GRIK1;GRIN3A;GRIN2A;GRIA4; GRIK4;CNIH3;UNC13A;GRM8;GRIA1; GRM3;GRIK3;GRIA2	9.1E-10	0.006915
extracellular matrix organization	0030198	329	57	17	ADAMTS3;BMP4;TNXB;ADAMTS20; COL1A1;AGRN;NPHP3;ADAMTS2;DMD; DSPP;BMP2;PDGFRA;TIMP2;MMP2; B4GALT1;COLGALT2;LTBP1;TNR; COL17A1;KLK7;COL6A5;COL6A6;NID1;	2.79E-07	0.018756

					COL23A1;MMP16;LAMC2;COL5A2; COL6A3;LAMB1;ITGA11;COL25A1; MATN1;LAMA5;DCN;ITGB5;ITGB3; FOXF2;CD47;GFAP;NRXN1;PLOD2; COL22A1;EGFL6;C6orf15;SPINT1; COL11A1;COL27A1;CRISPLD2;BMP7; SMOC2;TLL1;THBS1;FBN2;RXFP1;ATP7A; COL2A1;ITGA6		
regulation of membrane potential	42391	91	24	26	ACTN2;KCNH8;KCNH1;ATP1A4;GRIK2; DMD;DLD;KCNMA1;HCN3;HCN1; CHRNA7;KCNJ11;CACNA1H;XIRP1;GRIK1; GRIN2A;CNIH3;NEDD4L;NEDD4;POPDC2; GRIK3;CHRNG;CNGB3;CACNA1A	4.92E-07	0.008469
adherens junction organization	34332	40	15	37	CDH2;CDH15;CDH5;CDH8;PVRL2;PVR; CDH4;DSP;CDH13;CADM2;CDH6;CDH9; CDH18;CDH7;MLLT4	5.08E-07	0.005372
transport	0006810; 0015460; 0015457	1853	219	11	OSBPL11;SCFD2;SYT10;RPH3A;ANO4; ANO3;SCP2;ATP1A4;PAFAH1B1;SLC26A3; CATSPER3;EXOC2;IGF2R;KPNA6;CHRNA7; SLC3A1;ABCG2;RANBP17;IPO11;ATP8B2; SYT6;CACNA1H;DYNC1LI1;SLC19A1; SLC25A4;GRIK1;FKBP15;GRIN2A;GRIA4; GRIK4;CACNG3;OSBPL3;ESYT3;PDCD6IP; CNNM2;SARAF;LRRC38;SLC22A5;SORT1; XPO7;AP5M1;DYNC1I2;AP4M1; DENND2A;VPS53;IPO5;GLE1;NUP210; SLC16A8;PGAP1;ABCA1;ALB;CHMP1A; RABEP2;ABCB11;SMAD3;KPNA3;AGAP1; ABCA9;ABCA13;ARL4C;RAB3B;ETFA; STARD3;FDXR;PARP4;FABP5;SLC44A1;	5.64E-07	0.049761

					SNX33;SPNS1;SPNS2;CHP2;RYR2; CACNA1C;NDUFS4;PCLO;ABCB4;DYNLT3; ABCB1;FDX1;CACNA1A;ATP7A;KCNN4; SLC22A1;RYR3;CYBRD1;SLC15A3; TMEM30B;SLC16A7;ATP2C2;ABCC5; TPCN2;SLC5A8;NALCN;SLC24A3; TOMM40;FXYD4;SLC39A10;SLC12A7; SLC12A3;SLC15A5;SLC6A9;SLC9A7; SLCO3A1;SLC15A1;RUFY1;KCNH8;KCNH1; LASP1;SLC16A6;ABCC2;SLC39A8; SLC40A1;SLC25A18;SLC13A1;LBP; ATP12A;SLC22A23;SLC4A11;CLIC6;BEST3; PEX14;KIF16B;TMEM38B;KCNE3;KCNIP4; AP3S1;AP3B1;CACNA2D3;PKD1L1; CACNA2D1;LRPPRC;LCA5;SLC36A4; GRIK2;GRIN2B;PMP2;KIF17;LSG1; TOMM7;PANX3;KCNQ5;KCNMA1;KCNA4; KCNK9;HCN3;KCNAB1;KCNJ6;SLC22A2; SLC6A1;HCN1;KCNC4;KCNF1;KCNA3; SLC1A3;CACNB2;KCNJ11;KCNS3; KCNMB4;ATP1B4;RBP3;SLC31A2; CADPS2;ERGIC2;SLC30A8;SCN5A; OSBPL1A;CLCN1;KCNJ3;KCND2;TXNL1; PEX12;LIN7B;ICA1;SYNRG;SYT1;STX3; GOSR2;VTI1A;RAB9B;RAB7A;SLC35F2; SLC35F1;TTPAL;ERGIC3;MFSD2B;CLIC5; TRPC7;XK;TMEM106B;SNX10;PTPN23; CUBN;TRPM7;COG6;GC;TMED10;APOM; DUOXA1;GJA1;SLC8A1;FA2H;RAMP1; ITPR1;VPS54;MIA3;STEAP3;CCDC64;		

					RAB2A;CLIC1;CNIH1;GRIK3;CHRNG; GABRD;RHCG;CNGB3;RAMP3;JAKMIP1; GRIA2		
ionotropic glutamate receptor signaling pathway	35235	27	12	44	CPEB4;GRIK2;GRIN2B;GRIK1;GRIN3A; GRIN2A;GRIA4;GRIK4;FYN;CAMK2A; GRIK3;GRIA2	8.19E-07	0.004313
potassium ion transmembrane transport	71805	134	30	22	KCNN4;SLC24A3;FXYD4;SLC9A7;KCNH8; KCNH1;TMEM38B;KCNT2;KCNE3; KCNK12;KCNIP4;ATP1A4;KCNQ5; KCNMA1;KCNA4;KCNK9;HCN3;KCNAB1; KCNJ6;HCN1;KCNC4;KCNF1;KCNA3; KCNJ11;KCNS3;KCNMB4;KCNJ3;KCND2; SLC24A2;CNGB3	9.33E-07	0.010449
potassium ion transport	0015458; 0006813	136	30	22	KCNN4;SLC24A3;SLC12A7;SLC9A7; KCNH8;KCNH1;ATP12A;TMEM38B; KCNT2;KCNE3;KCNIP4;ATP1A4;KCNQ5; KCNMA1;KCNA4;KCNK9;HCN3;KCNAB1; KCNJ6;HCN1;KCNC4;KCNF1;KCNA3; KCNJ11;KCNS3;KCNMB4;ATP1B4;KCNJ3; KCND2;SLC24A2	1.30E-06	0.010442
skeletal system	48705	59	18	30	TFAP2A;COL1A1;CSRNP1;PDGFRA;SCHIP	1.31E-06	0.00641
cell junction assembly	34329	77	21	27	CDH2;CDH15;CDH5;CDH8;PVRL2;PVR; COL17A1;LAMC2;CDH4;GRHL2;INADL; CDH13;CLDN17;CADM2;CDH6;CDH9; CDH18;CDH7;RSU1;ITGA6;MLLT4	1.38E-06	0.007439
cell-cell junction organization	45216	71	20	28	CDH2;CDH15;CDH5;CDH8;PVRL2;PVR; NLGN4X;CDH4;SMAD3;GJA1;INADL; CDH13;HNF4A;CLDN17;CADM2;CDH6;	1.41E-06	0.007097

					CDH9;CDH18;CDH7;MLLT4		

Supplementary Table S5. Enriched '*biological process'* gene ontology (GO) terms associated with scar pliability (SP) (*P*<1.68E-06; Bonferroni correction for multiple pathways). Gene regions imported into Pathway Studio® were identified as those with at least two SNP sites and *P*-value <0.01.

Name	**GO ID**	**# of Entities**	**Overlap**	**Percent Overlap**	**Overlapping Entities**	***P*-value**	**Jaccard similarity**
cell adhesion	0007155	616	116	18	EPHA4;PLCB1;KITLG;CD151;EDIL3;CDH2; TSPAN5;CDH3;SDC1;CADM1;CDH5; EPHB1;AMICA1;LAMA1;PVRL2;CD2; CXADR;PPAP2B;TYRO3;AZGP1;APP; CDH17;PCDH8;SIGLEC6;SVEP1;KIAA1462; SDK1;LAMB4;LPP;CDH20;PCDH19;DSG1; PCDH10;AJAP1;DSC1;CTNNA3;HAS2; CLSTN2;ITGB8;DSC3;NINJ2;IGSF11; PARVA;RAC1;NFASC;CNTNAP2;SORBS2; FAT1;EMP2;RPSA;PCDH15;CHST10; MYBPC1;VCAM1;DSG3;CNTNAP4; COL6A5;CNTN4;TLN2;CTNNA2;AMIGO2; DSCAML1;LEF1;ROBO1;ITGA11;CDH11; ACAN;SEMA5A;FBLN5;STAB2;SCARB1; CDH4;DSCAM;COL14A1;CELSR1;FAT3; GRHL2;LSAMP;ARHGAP5;ADAM22; SPOCK1;RELN;NRXN1;FLRT2;ABL1;DPT; CDH13;OLFM4;NCAM2;NTM;CDH12; CADM2;CDH6;CDH7;CTNND2;NEDD9; PTPRT;CD34;PTPRM;RGMB;LRRN2; TENM2;PLXNC1;PRKCE;TENM3;MPZL2; PTPRF;ALCAM;RADIL;CDH1;LGALS3BP; CNTN5;CNTNAP5;CSF3R;ITGA6;LPXN	1.68E-20	0.038978
nervous system	0007399	523	98	18	EPHA4;EPM2A;GFRA1;GFRA2;TNIK;DPF3;	2.42E-17	0.033781

development					ERBB4;MEF2A;RAPGEF2;LMTK2;RTN4; EFNA5;SRGAP2;APOB;EPHB1;PAFAH1B1; IFT88;PTPRR;EPHA7;NAV1;APP;GATA3; SLIT3;NOVA1;PPT1;DLG2;KDM7A;APBA2; VEGFA;NRSN1;SRGAP2B;SEMA3A;LPPR1; MOBP;HDAC4;HDAC9;PRKD1;NINJ2; CSRP1;GRIK1;MYO1B;PEX2;CNTN4; ARHGAP26;NRN1;NTNG1;DSCAML1; FEZF2;PTPRO;ROBO1;ATOH1;MPPED2; ST8SIA2;BTBD3;DCX;GRIP1;INTU;DAB1; RAPGEF5;GMFB;NDNF;SEMA5A;DSCAM; LHX2;SEMA3E;NELL1;PCSK2;CRX;OLIG2; LBX1;OLFM1;LSAMP;SPOCK1;PLXNA4; RGS9;DYRK1A;ASCL1;SRRM4;KIAA1279; NEUROD2;SEMA3D;MEF2D;CHRM3; SCN2A;MYT1L;ARID1B;BRSK2;MDGA1; FNBP1;HELT;PTPRF;MAGI2;CER1;NAV2; DACT1;GDA;DPYSL2;SOX11		
multicellular organismal development	0007275	1171	153	13	PLXDC2;CCBE1;FOXL1;DMRT1;EPHA4; DAZL;TNFRSF11A;DIXDC1;TNP1;DNER; FGF4;SPRED2;SFRP2;SHB;QKI;DPY19L2; ERBB4;EDIL3;MEF2A;RAPGEF2;SPIN1; MKX;PIWIL1;GTF2IRD1;FLT1;TSHZ2; LRIG3;KIAA1217;HLF;TMEM2;FRAT2; FMN2;SHISA3;MAK;PRM1;EFNA5; DYNC2H1;KIF26B;TLE3;RFX3;JAG2;ICK; PDGFC;CADM1;SLC22A16;NOTCH4; KCTD15;STRBP;BMP5;PAFAH1B1;EPHA7; CATSPER3;DIAPH2;PPAP2B;HOXA11; NAV1;MITF;PITX2;GFI1B;JARID2;TBX5;	8.2E-12	0.043789

					SFRP1;SLIT3;KDR;VEGFA;PDGFD;SOX3; SEMA3A;HOXD9;KRT8;SHROOM3; ZBTB18;CSF3;SORT1;CTNNA2;NTNG1; FEZF2;ROBO1;ATOH1;LSM14A;DCX;INTU; DAB1;SEMA5A;EMP1;ST6GAL2; NKX2-5;CELSR1;SEMA3E;SOX6;FAT3; EOMES;HHEX;IRX3;CRX;OLIG2;LBX1; OLFM1;PLXNA4;RELN;IKZF1;EYA4;EYA1; WLS;ASCL1;FZD3;FOXA1;TAL1;ISL1; LMX1B;CTNND2;TMEM100;UNC5C;STIL; ARHGAP22;RYR2;KIAA1279;ZNF521; NEUROD2;PKDCC;SEMA3D;MEF2D; MYT1L;ARHGAP24;MDGA1;HELT;TENM4; G2E3;PLXNC1;HOXC4;FGF3;GSC; NKX3-1;NXN;RADIL;GLI3;EID2;MEIS2; DACH2;RBM19;HOXD8;DACT1;CASZ1; PLXNA2;EBF2;ZFP64;PBX1;PHOX2B; PITX1;SPRY2;DPYSL2;SOX11;EDARADD		
synaptic transmission	0007268	472	79	16	PLCB1;RPS6KA2;ADCY2;GABRG3;SSTR4; HTR2A;HAP1;SSTR1;GRIK2;NPFFR2; PAFAH1B1;DRD1;PCDH8;DLGAP1;KCNQ3; KCNMA1;KCNS2;NOVA1;KCNJ4;NRXN3; PPT1;KCNAB1;KCNJ6;KCNV1;GAD1; KCNA2;HCN1;CACNA1E;SLC1A6;GABRB1; DLG2;APBA2;MBP;GLS;SV2C;NPY5R; SLC1A3;KCNA6;CLSTN2;PPFIA2;KCNS3; ASIC2;KCNA1;ABAT;TACR1;GRIK1; GRIN2A;GRIA3;GRIA4;GRIK4;CACNG4; KCNJ3;KCND2;RIMS1;MYO5A;GRIP1; AP2B1;PDE7B;NRXN1;GNAI1;GABRB3;	1.34E-11	0.027536

					CAMK2A;KCNK2;GPR139;GABRB2; KCNA5;GRM3;ADCY1;NCALD;GRIK3; CHRM3;OPRD1;HTR7;HTR4;DTNA; CHRNB2;GALR1;UNC13C;HOMER1		
homophilic cell adhesion via plasma membrane adhesion molecules	0007156	161	39	24	CDH2;CDH3;PCDH9;CADM1;CDH5;PVRL2; CDH17;PCDH8;CDH20;PCDH19;DSG1; PCDH10;DSC1;PCDH7;CDH19;DCHS2; CLSTN2;DSC3;FAT1;PCDH15;DSG3; AMIGO2;DSCAML1;ROBO1;CDH11;CDH4; CELSR1;FAT3;CDH13;CDH12;CDH6; CDH18;CDH7;PTPRT;PTPRM;TENM3; MPZL2;PTPRF;CDH1	4.32E-11	0.015012
positive regulation of transcription from RNA polymerase II promoter	0045944; 0045817; 0010552	1041	137	13	TRAF6;DMRT1;HDGFL1;MOSPD1;GLI2; IL17F;NFATC2IP;FGF4;CD3D;SFRP2;ELK3; TFAP2A;MEF2A;AIRE;MAP2K5;MKX; DICER1;RBPJ;ZNF133;SOX17;RFX3;PARK2; GDF2;BMP5;KLF4;KLF6;ETV5;MITF;PITX2; APP;IL17A;ASXL2;NCOA2;GATA3;TBX5; RUNX1;SMYD3;VEGFA;ADRB2;ETS1;FLI1; MAML2;MAML3;FSHB;NCOA3;ZMIZ1; PARK7;PPARGC1A;HOXD9;NOS1;HDAC4; TBL1XR1;SALL1;SKI;PRKD1;ABLIM2; ABLIM3;DAXX;CSF3;DHX36;MYC;TET1; PIK3R1;NR5A2;REST;LEF1;ETV1;TFAP2D; ATOH1;RORA;ONECUT2;SMAD2;MAF; HIPK2;SMAD3;NKX2-5;LHX2;SOX6;KLF2; NFIA;EOMES;BCL11B;HHEX;CRX;MEIS1; NPAS2;PTH;TNKS;IKZF1;EYA1;CDH13; ASCL1;FOXA1;TAL1;ISL1;LMX1B;CDK8; FGFR2;E2F7;NFATC1;GATA5;RLF;OSR1;	6.6E-11	0.040533

					NFATC4;LDB2;ZFPM2;NEUROD2;ELF4; MEF2D;NRF1;MYT1L;ETV6;PPARG;SPIC; HELT;WWOX;GLIS3;PBX2;PLAGL1; NKX3-1;GLI3;MEIS2;KLF13;RUNX2;JADE1; HOXD8;TLX1;GALR1;NAMPT;EBF2;PBX1; PHOX2B;PITX1;IL33;ZFAT;SOX11;ITGA6		
axon guidance	0007411; 0008040	385	66	17	EPHA4;GLI2;RPS6KA2;GFRA1;CLASP2; LMTK2;EFNA5;SRGAP2;MYO10;EPHB1; LAMA1;EPHA7;GATA3;SLIT3;KCNQ3; NRXN3;SEMA3A;MMP2;SPTBN4;ABLIM2; RAC1;ABLIM3;EPHA6;NFASC;VAV3; CNTN4;FEZF2;COL4A2;COL5A2;ETV1; PTPRO;ROBO1;B3GNT2;ATOH1;TRPC7; ST8SIA2;COL4A1;RGMA;DCX;TTC8; SEMA5A;AP2B1;CDH4;MYH11;LHX2; SEMA3E;PLXNA4;KIF4B;ITSN1;RELN; NRXN1;FLRT2;ABL1;RGMB;UNC5C; TENM2;EXT1;PLXNC1;ALCAM;GLI3; PLXNA2;DOCK1;SPTBN1;ANK3;DPYSL2; COL2A1	2.3E-10	0.023614
cell-cell junction organization	0045216	71	23	32	CDH2;CDH3;CADM1;CDH5;PVRL2;CXADR; PARD3;CDH17;XIRP2;RAC1;NLGN4X; CDH11;CDH4;SMAD3;INADL;CDH13; CLDN17;CDH12;CADM2;CDH6;CDH18; CDH7;CDH1	9.62E-10	0.009113
cell junction assembly	0034329	77	23	29	CD151;CDH2;CDH3;CADM1;CDH5;PVRL2; PARD3;CDH17;PARVA;CDH11;CDH4; GRHL2;INADL;CDH13;CLDN17;CDH12; CADM2;CDH6;CDH18;CDH7;RSU1;CDH1; ITGA6	5.69E-09	0.009091

single organismal cell-cell adhesion	0016337	145	33	22	BCL2;EMCN;CDH2;CDH3;CDH5;FNDC3A; ICOS;CD2;CXADR;PPAP2B;PARD3;DSG1; CTNNA3;FAT1;RPSA;KIRREL;VCAM1; CTNNA2;CDH11;COL14A1;LSAMP;CDH13; NTM;CDH7;CTNND2;CD34;DLG5;TENM2; VNN1;MPZL2;CDH1;PKHD1;ITGA6	7.16E-09	0.012751
regulation of membrane potential	0042391	91	25	27	TRPM4;GRIK2;DMD;DLD;KCNMA1;HCN1; SLC1A6;ASIC2;KCNA1;GRIK1;GRIN2A; SCN1A;DPP6;PEX5L;NEDD4L;RIMS1; NEDD4;POPDC2;KCNK2;KCNA5;GRIK3; ABCB5;CNGB3;CHRNB2;CNGB1	8.4378E-09	0.009834776
signal transduction	0007165; 0023033	1843	207	11	PLCB1;PDE3A;RPS6KA2;KITLG;RXFP2;SHB; FSHR;TAAR1;ELK3;SMC3;ADCY2;TRPM1; GABRG3;ARAP2;CSNK1G3;TLE3;SSTR1; RAN;PVRL2;LGR5;TYRO3;DRD1;MTNR1A; NCOA2;NPAS3;GABRB1;NPY5R;ADRB2; ANXA1;FSHB;NOS2;ZP2;P2RX1;AVPR1A; TACR1;RIPK3;BTRC;PIK3R1;VAPA;NPAS2; CRY1;NEDD9;IGF1R;NEK6;PPP2R2D; PRKCE;MAGI2;ANK3;TRAF6;TNFRSF11A; FFAR4;FGF4;SFRP2;PAK4;ERBB4;ITPKB; RAPGEF2;MAP2K5;DOK2;MAP2K4; ADRA1A;SSTR4;HTR2A;SRGAP2;ICK; PTGER4;GRIK2;SYNGAP1;NPFFR2;EPHA7; TNFRSF10A;GATA3;NCOA3;PRKD1;DLC1; CDC42EP3;YWHAZ;ARHGAP26;IQGAP2; GMFB;CELSR1;HHEX;SOCS3;RGL1;PDE7B; SPOCK1;ARHGAP42;CD274;PLXNA4; RAMP1;TNFRSF11B;ITPR1;SRGAP3; GNAI1;STARD13;PTCH1;FZD3;NMU;	1.19959E-08	0.050340467

					ANXA5;GNL1;CTNND2;INPP4B;SPARCL1; GPR174;GABRB3;RASA2;PTPRT;CD34; CBLB;PTPRM;PROKR2;RGMB;UNC5C; LRRN2;ARHGAP20;GPR139;GABRB2; LRP12;RGS5;GRM3;GUCY1A2;SMOC2; ADCY1;CNIH1;ARHGAP22;PLCXD3; PTGER3;HIVEP2;GPRC5B;GRIK3;CHN2; DLG5;ITPR2;CHRM3;TENM2;TNFSF18; GAST;OPRD1;OSTF1;PDCL;IL15RA; ARHGAP24;MC3R;GPR158;PPARG; HLA-DOA;TAS2R5;HTR7;TENM4;HINT1; OR8B2;GRB14;RSU1;EXT1;PLXNC1; CNGB3;RASL11B;MPZL1;RAMP3;TENM3; MYO9B;IL15;PLCL2;GRB10;HTR4;OR7A17; STAP1;DTNA;FGF3;PTH2R;PTPRF;ALCAM; GRP;RADIL;EXT2;PTCHD4;ASB2;CHRNB2; MC4R;LGALS3BP;GRK5;RGS12;RASA3; GPR45;GALR1;OR2F1;UNC13C;CSF3R; PLXNA2;RALGDS;NAMPT;TRHR;XCL1; DOCK1;MRGPRX1;LGALS9;NCR1;AGTR1; CDC42SE2;RPS6KC1;DPYSL2;IRS2;LPXN; EDARADD;FASLG;QRFPR;CCK		
ion transport	0006811	627	87	13	STEAP4;SLC6A15;ASIC5;SLC22A24; SLC5A8;ATP2A3;SLC39A10;SCNN1A; SLC4A4;SLC9A9;SLC10A7;SLC4A3; SLCO3A1;SLC38A4;SLC22A8;TRPM1; GABRG3;P2RX7;LASP1;CLCN4;SLC15A2; TRPM4;SLC17A6;SLC22A23;KCNIP4; ATP6V0D2;ATP6V1C1;ATP6V0E1;ORAI1; SLC22A16;CLCA1;GRIK2;SLC7A2;SLC26A3;	1.97643E-08	0.028846154

					CATSPER3;KCNQ3;KCNMA1;KCNS2; KCNJ4;KCNAB1;KCNJ6;KCNV1;KCNA2; HCN1;CACNA1E;SLC1A6;GABRB1;SLC1A3; KCNA6;KCNS3;ASIC2;KCNA1;SCARA5; P2RX1;SLC30A8;GRIK1;GRIN2A;GRIA3; GRID1;GRIA4;GRIK4;CACNG4;CLCN1; CNNM2;KCNJ3;KCND2;SLC24A2;ADD2; CLIC5;TRPC7;SLC22A4;SLC3A2;SLC39A3; SLC8A1;ITPR1;ATP5O;GABRB3;KCNK2; GABRB2;KCNA5;RYR2;GRIK3;ITPR2; CNGB3;CHRNB2;SLC24A5;SLC12A2		
cell differentiation	0030154	849	107	12	DMRT1;GLI2;DNER;FGF4;SFRP2;SHB;QKI; DPY19L2;ELK3;TGFBR2;MEF2A;MEIG1; RAPGEF2;PIWIL1;FLT1;MAK;PRM1; SPATA31D1;EFNA5;TLE3;RFX3; SPATA31C2;JAG2;USP42;CADM1; SLC22A16;NOTCH4;GALNTL5;STRBP; BMP5;PAFAH1B1;KLF4;CATSPER3; BMPR1B;ETV5;PARD3;NAV1;MITF; JARID2;SFRP1;SLIT3;KDR;VEGFA;ETS1; FLI1;SEMA3A;PRKD1;SORT1;CTNNA2; SRPK2;NTNG1;FEZF2;ETV1;ROBO1; ATOH1;DCX;ONECUT2;DAB1;SEMA5A; NKX2-5;SEMA3E;EOMES;HHEX;NELL1; CRX;LBX1;TMTC3;ABL1;ASCL1;TAL1; TMEM100;OSR1;NFATC4;ARHGAP22; SRRM4;ZFPM2;KIAA1279;ZNF521; NEUROD2;PKDCC;SEMA3D;ELF4;MEF2D; PAPPA;TRAPPC9;ABCB5;MYT1L;ETV6; ETV3;THSD7A;ARHGAP24;MDGA1;SPIC;	8.49638E-08	0.033250466

					FNBP1;HELT;TENM4;TENM3;PLAGL1; FGF3;NXN;EXT2;PRDM16;EID2;PBX1; DPYSL2;SOX11;EDARADD		
adherens junction organization	0034332	40	15	37	CDH2;CDH3;CADM1;CDH5;PVRL2;CDH17; CDH11;CDH4;CDH13;CDH12;CADM2; CDH6;CDH18;CDH7;CDH1	8.6996E-08	0.005997601
glutamate receptor signaling pathway	0007215	14	9	64	PLCB1;SSTR1;GRIK2;GRIK1;GRIN2A; GRIA3;GRIA4;GRIK4;GRIK3	1.06693E-07	0.00362757
negative regulation of cell proliferation	0008285	471	68	14	RPS6KA2;BCL2;SFRP2;RXFP2;GPLD1; ERBB4;TGFBR2;TFAP2A;RAPGEF2; ADRA1A;IGFBP3;SSTR4;RBPJ;SLFN12L; TNFRSF9;SSTR1;CDH5;BMP5;KLF4; ZBTB16;AZGP1;JARID2;GATA3;TBX5; RUNX1;SFRP1;SLIT3;KISS1;ETS1;ABI1; TIMP2;NOS1;HDAC4;SKI;DLC1;SCIN; BAK1;FEZF2;REST;ROBO1;SMAD2; SMAD3;BCL11B;GTPBP4;LBX1;SMAD6; ATP8A2;BRIP1;DPT;ING1;CDH13;CTH; PTCH1;SH3BP4;FGFR2;E2F7;PTPN14; DLG5;SOD2;PPARG;PTPRF; NKX3-1;MAGI2;CER1;GLI3;KLF13; PHOX2B;SPRY2	1.56514E-07	0.023619312
intracellular signal transduction	0007242; 0007243; 0023034; 0023013; 0035556	519	73	14	DMRT1;CD3E;PLCB1;RPS6KA2;DUSP1; TNIK;PAK4;ADCY2;RAPGEF2;KSR1; ADRA1A;KSR2;FMN2;ICK;RP1;ADCY10; TESK2;NOS2;PRKD1;RAC1;NRG3;SYK; VAV3;SRPK2;DCX;GRIP1;DCDC5;AKAP6; DEPTOR;RGS7;SMAD2;DAB1;RAPGEF5;	1.58666E-07	0.024982888

					PLCB4;SPATA13;GAB2;ASB5;SMAD3; INSR;SOCS3;RGS6;PDK1;SMAD6;ITSN1; ASB3;PIKFYVE;DEF8;FLRT2;MKNK1;TLK1; PREX2;DCDC1;DCLK2;INADL;RGS9;RASA2; CBLB;NFATC1;GUCY1A2;ADCY1;CNIH1; CHN2;DLG5;PDCL;GRB14;PRKCE;MYO9B; PLCL2;ASB2;RGS12;RASA3;UNC13C;NCR1		
negative regulation of transcription from RNA polymerase II promoter	0010553; 0045816; 0000122	799	101	12	TRAF6;DMRT1;HDGFL1;TRIM29;MOSPD1; GLI2;KLF17;FST;TFAP2A;MEF2A;ZNF536; MAP2K5;MKX;DICER1;RBPJ;TLE4;KDM2B; SOX17;KLF4;ZBTB16;MITF;PITX2;GFI1B; JARID2;ASXL2;NCOA2;GATA3;CREBRF; VEGFA;NCOR2;SOX3;HOXD9;HDAC4; HDAC9;BRMS1L;TBL1XR1;PRDM5;SALL1; SKI;TRPS1;DAXX;ZBTB18;MYC;PEX2; NEDD4L;FEZF2;REST;LEF1;SMAD2;MAF; SP100;HIPK2;SMAD3;NKX2-5;SOX6;NFIA; EOMES;HHEX;OLIG2;PTH;IKZF1;MTDH; PTCH1;ASCL1;FOXA1;TAL1;ISL1;CRY1; WWC2;FGFR2;E2F7;NFATC1;CCND1; OSR1;NFATC4;LMCD1;ZFPM2;TBX15; ZMYND8;MLIP;TENM2;ETV6;ETV3; PPARG;HELT;GLIS3;URI1;GSC;GLI3; PRDM16;H2AFY;EID2;MEIS2;HOXD8; DACT1;TCF25;OLIG3;GCFC2;PKIA;SOX11; FASLG	1.70203E-07	0.031821046
negative regulation of cell proliferation	0008285	471	68	14	RPS6KA2;BCL2;SFRP2;RXFP2;GPLD1; ERBB4;TGFBR2;TFAP2A;RAPGEF2; ADRA1A;IGFBP3;SSTR4;RBPJ;SLFN12L; TNFRSF9;SSTR1;CDH5;BMP5;KLF4;	3.8328E-07	0.023619312

					ZBTB16;AZGP1;JARID2;GATA3;TBX5; RUNX1;SFRP1;SLIT3;KISS1;ETS1;ABI1; TIMP2;NOS1;HDAC4;SKI;DLC1;SCIN; BAK1;FEZF2;REST;ROBO1;SMAD2; SMAD3;BCL11B;GTPBP4;LBX1;SMAD6; ATP8A2;BRIP1;DPT;ING1;CDH13;CTH; PTCH1;SH3BP4;FGFR2;E2F7;PTPN14; DLG5;SOD2;PPARG;PTPRF;NKX3-1; MAGI2;CER1;GLI3;KLF13;PHOX2B;SPRY2		
transmembrane transport	0055085	805	100	12	CYBRD1;SLC6A15;ASIC5;SLC16A7; MYO5B;SLC22A24;SLC5A8;ATP2A3; SLC2A12;SLC39A10;SCNN1A;SLC4A4; SLC15A5;SLC9A9;TRPM3;SLC6A9; SLC10A7;SLC4A3;BCL2;SLC37A1; SLCO3A1;SLC38A4;SLC22A8;ADCY2; TRPM1;GABRG3;CETP;CLCN4;SLC37A3; SLC15A2;TRPM4;SLC17A6;SLC22A23; ATP2B4;SGK1;TRDN;APOB;ANO5;ANO4; ANO3;ANO10;ATP6V0D2;ATP6V1C1; ATP6V0E1;SLC22A16;CLCA1;OCA2; SLC7A2;SLC26A3;CATSPER3;KCNQ3; KCNMA1;KCNS2;KCNAB1;KCNV1;KCNA2; HCN1;CACNA1E;SLC1A6;GABRB1;SV2C; SLC1A3;KCNA6;KCNS3;ASIC2;KCNA1; SLC30A8;CLCN1;NUP35;KCND2;SLC24A2; NEDD4L;SLC18A1;SLC25A21;TRPC7; ABCA1;SLC22A4;ALB;SLC3A2;SLC27A6; SLC39A3;GJC3;GJA3;SLC8A1;ITPR1; SLC44A1;GABRB3;GABRB2;KCNA5;SPNS1; SPNS2;GCK;ADCY1;RYR2;ITPR2;ABCB4;	4.46486E-07	0.031436655

					ABCB5;CNGB3;SLC24A5;SLC12A2		
sensory perception of sound	0007605	157	31	19	TFAP2A;JAG2;DIAPH1;KCNMA1;SLC1A3; SPTBN4;ASIC2;OTOR;PCDH15;SLITRK6; CLIC5;GJC3;ALG10;EYA4;EYA1;GABRB3; USH2A;GABRB2;SRRM4;SOD2;NAV2; CHRNB2;CDH1;LRIG1;FAM107B;TECTA; TECTB;CNTN5;MYO15A;SPRY2;COL2A1	6.03513E-07	0.011913912
regulation of ion transmembrane transport	0034765	191	35	18	TRPM4;KCNT2;KCNK12;KCNIP4; CATSPER3;KCNQ3;KCNMA1;KCNS2; KCNJ4;KCNAB1;KCNJ6;KCNV1;KCNA2; HCN1;CACNA1E;KCNA6;KCNS3;ASIC2; KCNA1;GRIK1;GRIN2A;CACNG4;CLCN1; SCN1A;KCNJ3;KCND2;NEDD4L;CLIC5; REST;NEDD4;NCS1;KCNK2;KCNA5;SCN2A; CNGB3	7.58438E-07	0.013297872
locomotory behavior	0007626	108	24	22	FSHR;PARK2;ETV5;DRD1;APP;NOVA1; NPAS3;CACNA1E;APBA2;ABAT;GRIN2A; PCDH15;FEZF2;GMFB;DSCAM;CELSR1; FIGN;RELN;TAL1;GPRC5B;SOD2;NAV2; CHRNB2;MYO15A	1.2303E-06	0.009375
ion transmembrane transport	0034220	291	46	15	ASIC5;SLC22A24;ATP2A3;SCNN1A; TRPM3;SLC4A3;SLCO3A1;SLC22A8; TRPM1;GABRG3;LASP1;CLCN4;TRPM4; ATP2B4;SGK1;TRDN;ANO5;ANO4;ANO3; ANO10;CLCA1;GRIK2;SLC26A3;SLC1A6; GABRB1;ASIC2;GRIK1;GRIN2A;GRIA3; GRID1;GRIA4;GRIK4;CLCN1;SLC24A2; NEDD4L;TRPC7;ABCA1;SLC22A4;TPTE2; GABRB3;GABRB2;RYR2;GRIK3;CHRNB2; SLC24A5;CNGB1	1.2934E-06	0.016905549

response to drug	0042493; 0017035	509	69	13	PDE3A;BCL2;SFRP2;ERBB4;TGFBR2; GABRG3;P2RX7;ADRA1A;ALAD;HTR2A; CDH3;PARK2;REN;DRD1;GATA3;SFRP1; GAD1;KDR;CCNE1;SLC1A3;ALDH1A1; ANXA1;TIMP2;MMP2;PARK7;LPL; PPARGC1A;HDAC4;AOC1;ABAT;AACS; OXCT1;DPYD;GRIN2A;MYC;VAV3;GMPS; PIK3R1;YWHAZ;BAK1;HADH;ABCA1; DAB1;OGG1;SOCS3;SLC8A1;CPS1;PTH; DAD1;TNFRSF11B;RELN;MGMT;ABL1; CST3;PTCH1;FZD3;PARP4;TGFA;PTPRM; CCND1;ADCY1;RYR2;ABCB4;SOD2; PPARG;CDH1;GRK5;FECH;DPYSL2	1.3459E-06	0.023662551